1181

Institut de physique
Université de Neuchâtel

PREPARATION ET CARACTERISATION DE COUCHES MINCES ET DE RESEAUX SUPRACONDUCTEURS A HAUTE TEMPERATURE CRITIQUE

Forme réduite de la
THESE

présentée à la Faculté des Sciences
de l'Université de Neuchâtel
pour l'obtention du grade de docteur ès sciences

par
Ph. Flückiger
physicien diplômé
de l'Université de Neuchâtel

Neuchâtel, décembre 1992

IMPRIMATUR POUR LA THÈSE

Préparation et caractérisation de couches minces et de réseaux supraconducteurs à haute température critique

de Monsieur Philippe Flückiger

UNIVERSITÉ DE NEUCHÂTEL

FACULTÉ DES SCIENCES

La Faculté des sciences de l'Université de Neuchâtel
sur le rapport des membres du jury,

MM. P. Martinoli, H. Beck, Ch. Leemann et O. Fischer (Genève)

autorise l'impression de la présente thèse.

Neuchâtel, le 10 août 1993

Le doyen :

A. Robert

PHYSICAL REVIEW B VOLUME 40, NUMBER 16 1 DECEMBER 1989

Critical phase fluctuations in superconducting wire networks

B. Jeanneret, Ph. Flückiger, J. L. Gavilano, Ch. Leemann, and P. Martinoli
Institut de Physique, Université de Neuchâtel, 2000 Neuchâtel, Switzerland
(Received 21 September 1989)

A study of the onset of superconducting phase coherence in periodic wire networks with weakly coupled adjacent nodes is presented. In a narrow temperature range below the mean-field critical temperature, ac conductance measurements reveal a drop in superfluid density and a peak in dissipation providing the first observation in networks of the vortex unbinding transition predicted by the Kosterlitz-Thouless theory. The ac response in the critical region is accurately described by dynamical extensions of the theory incorporating vortex-pinning phenomena created by the periodic structure of the network.

Networks of superconducting wires and arrays of Josephson weak links[1] prepared by modern lithographic techniques provide excellent systems to study fundamental concepts of condensed matter and statistical physics. Particularly attractive is the possibility of using these systems as testing grounds for the theoretical ideas of scaling, renormalization, frustration, and randomness underlying the physics of critical phenomena in two dimensions.

In this paper we explore the nature of the superconducting-to-normal (SN) transition (in zero magnetic field) of periodic two-dimensional (2D) wire networks[2] in the limiting case of weakly coupled nearest-neighbor nodes. Relying on a two-coil mutual-inductance method[3] to study the ac superfluid response of the system to a small oscillating driving field, we observe features in the critical region which provide strong evidence for a phase transition triggered by the vortex unbinding mechanism of the Kosterlitz-Thouless (KT) theory.[4] This conclusion is corroborated by a detailed study of the response based on dynamical extensions[5] of the KT theory. An important and distinctive aspect of our experiments, the fluctuating Brownian motion of vortex excitations in the periodic pinning potential created by the network, was included in the theoretical treatment and is shown to have a profound effect on the characteristic length scales probed in the ac measurements. The quality of the fit between theory and experiment emerging from our analysis is remarkable, comparable to that found so far only in studies of the superfluid transition in liquid-helium films[6] and in indium oxide films.[7] The results presented here are the first to show the KT transition in a network of superconducting wires. Previous work[2] on this system was performed in the strong-coupling regime, where the phase boundary in the (H,T) plane was found to be accurately described by the mean-field Ginzburg-Landau (GL) theory.

The nature of the SN transition of wire networks depends on the ratio a/ξ between the network lattice spacing a and the GL coherence length $\xi(T)$. Inspection of the GL free energy of the system[8] shows that for $a \ll \xi$ Josephson coupling between adjacent nodes is strong, the coupling energy being a factor $(2\xi/a)^2$ larger than the condensation energy in the interconnecting link. In this limit fluctuations in the phase ϕ_i of the complex order parameter at the nodal sites are irrelevant and the SN phase boundary of the network in the (H,T) plane is obtained by solving a linearized GL equation.[2]

The critical behavior of weakly coupled $(a \gg \xi)$ wire networks is radically different from that predicted by the mean-field GL approach. In this regime, below the mean-field critical temperature T_{co}, 2D phase fluctuations are essential to determine the nature of the SN transition, while amplitude fluctuations can be ignored. Assuming a position-independent order-parameter amplitude, which appears to be justified for $a \gg \xi$, the coupling energy of nearest-neighbor nodes takes on the piecewise parabolic dependence on $(\phi_i - \phi_j)$ characteristic of long $(a \gg \xi)$ microstrips with a piecewise linear current-phase relation.[9] The resulting expression of the free energy[8] shows that weakly coupled wire networks belong to the class of classical XY models with a temperature-dependent coupling energy given by[9]

$$E_J(T) = (\pi/4)(R_u/R_s)\Delta(T)\tanh[\Delta(T)/2k_BT],$$

where $\Delta(T)$ is the BCS gap parameter, R_s the normal-state strip resistance, and $R_u = \hbar/e^2$. According to the KT theory, the (zero field) critical behavior of the system is governed by 2D-phase fluctuations in the form of quantized vortices, the transition to the resistive state being driven by the unbinding of vortex-antivortex pairs at a critical temperature T_c lower than T_{co}.[9]

To ascertain this prediction, square wire networks with $a = 8$ μm containing about 10^6 nodes were photolithographically patterned from 200-Å-thick granular aluminum films. An appreciable reduction of T_c below T_{co} $(T_{co} - T_c \approx 100$ mK) and an $a/\xi(T_c)$ ratio of the order of 100 were obtained by an appropriate choice of the strip width $(w \approx 0.8$ μm) and of the normal-state resistivity of the Al films $(\rho \approx 150$ $\mu\Omega$ cm). The onset of 2D superconducting phase coherence in the networks was probed by studying their ac screening properties with an inductive technique.[3] The method consists of exposing the network to a weak ac magnetic field created by a 4-mm-diam drive coil located just above the sample. The excitation level, chosen to ensure a linear response, reached a maximum rms value of $\sim$0.4 mG at the center of the network, while ambient magnetic fields were suppressed to $\sim$1 mG. The response of the sample to the ac field was measured by

detecting the in-phase and quadrature components of the signal δV induced by the screening currents in a pair of astatic 2-mm-diam coils coaxially mounted within the drive coil. Data were taken at angular frequencies ω ranging from $\sim 6\times10^{3}\,s^{-1}$ to $\sim 6\times10^{7}\,s^{-1}$.

Figure 1 shows, emphasizing the critical-temperature region, the complex ac response $\delta V(T)$ measured at 10, 65, and 1000 kHz of an Al network with $R_s = 750\ \Omega$. Since the weak screening condition is almost satisfied at the temperatures of interest, $\delta V(T)$ is, to a first approximation, proportional to the complex ac conductance $G(T)$ of the sample.[3] In particular, $\mathrm{Im}[\delta V(T)]$ reflects the temperature dependence of the inverse kinetic inductance $L_K^{-1}(T)$ which measures the effective (renormalized) areal superfluid density in the network.[9] As shown in Fig. 1, in a narrow temperature range ($\Delta T \approx 30$ mK) centered about a frequency-dependent critical temperature T_ω we observe a marked drop in superfluid density, while a peak, whose position is used to locate T_ω, grows in the dissipative part $\mathrm{Re}[\delta V(T)]$ of the signal. These features are quite similar to those observed in ac measurements of the superfluid transition of other 2D systems[6,7,10,11] and as discussed in detail below, can be accurately described by dynamical theories[5] based on the KT vortex unbinding idea.

Also shown in Fig. 1 (upper part) is the dc resistive transition of the network. On the high-temperature side above T_{co}, fluctuations in the order-parameter amplitude lower the network sheet resistance below its normal-state value R_s. To obtain an estimate of T_{co}, the inverse excess conductance $(R^{-1}-R_s^{-1})^{-1}$ was fitted to the Aslamasov-Larkin theory[12] for fluctuation-induced superconductivity in two dimensions using T_{co}, R_s, and R_u as adjustable parameters.[7] From the fit, shown in the lower part of Fig. 1, we deduce $T_{co} = 2.236$ K, $R_s = 750\ \Omega$, and $R_u = 4.94$ kΩ (the theoretical value of R_u is 4.11 kΩ). The uncertainty in the determination of T_{co} is 25 mK.

The quantity to be compared with theory is the complex ac conductance rather than the signal voltage. Accordingly, G was calculated from the δV data by numerically solving the integral equation relating δV to G for our specific sample-coil configuration.[3] An example is shown in Fig. 2, where real and imaginary parts of ωG, as deduced from the 65-kHz response of Fig. 1, are plotted as a function of temperature and compared with the following prediction of the dynamical theory:[5,9]

$$G^{-1}(T,\omega) = [\omega L_{K0}(T)/\tilde{T}][\pi^4 y^2(l_\omega,\tilde{T}) + iK^{-1}(l_\omega,\tilde{T})] + R(\tilde{T})[a/\xi_+(\tilde{T})]^2, \quad (1)$$

where $L_{K0}(T) = (\hbar/2e)^2/E_J(T)$ is the kinetic inductance in the absence of thermal fluctuations. Equation (1) shows the decomposition of the network impedance G^{-1} in contributions from bound vortex pairs and from free vortices. The complex vortex-pair contribution is expressed in terms of two scale-dependent [$l \equiv \ln(r/a)$] and temperature-dependent [$\tilde{T} \equiv k_B T/E_J(T)$] quantities: the reduced stiffness K and the vortex excitation probability y. The characteristic length scale probed in the ac measurements is the vortex diffusion length $r_\omega \approx (14\mu k_B T/\omega)^{1/2}$, where μ is the vortex mobility discussed below in connection with thermally activated vortex motion in the periodic potential provided by the network. The renormalization procedure based on the Kosterlitz recursion equations[9,13] allows K and y to be computed for $l = l_\omega$ once their initial values at $l = 0$ are known. Adopting Mooij's notion,[9] we take $K(0,\tilde{T}) = \tilde{T}^{-1}$ and $y(0,\tilde{T}) = N_0 \exp(-2\pi\gamma/\tilde{T})$,

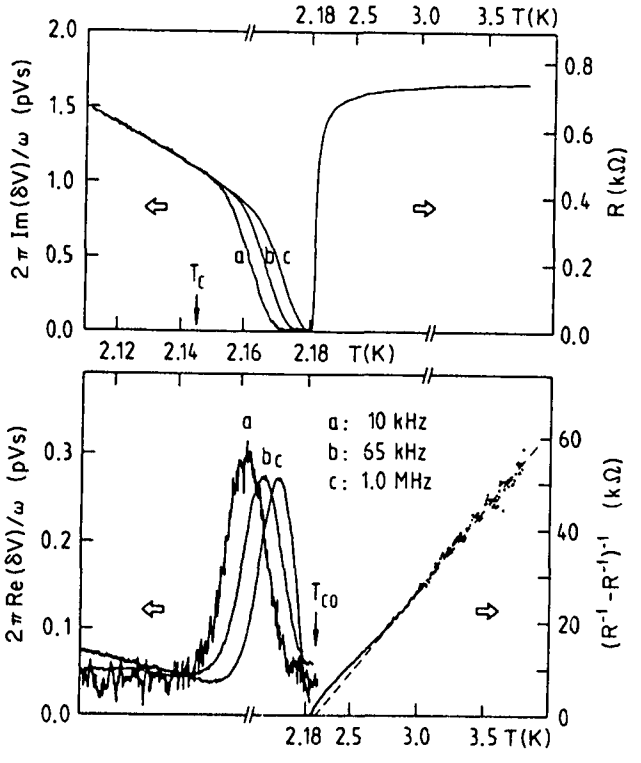

FIG. 1. Complex ac response vs temperature of a weakly coupled wire network measured at different frequencies near the superconducting transition. Also shown are the resistive transition (upper part) and the inverse excess conductance above T_{co} (lower part). The dashed line is a fit to the Aslamasov-Larkin theory.

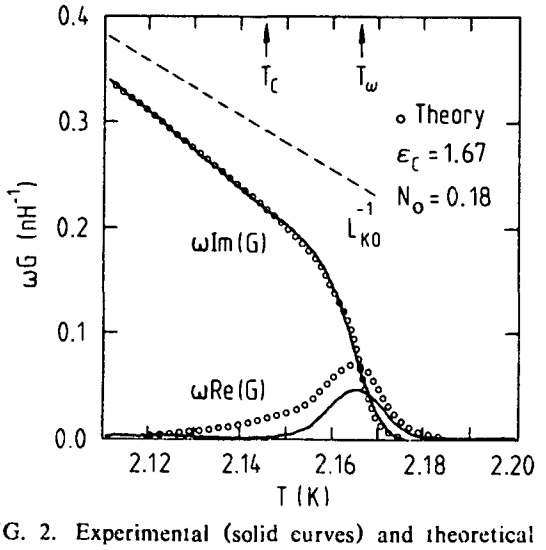

FIG. 2. Experimental (solid curves) and theoretical (open circles, see text) complex ac conductance at 65 kHz of the network of Fig. 1 as a function of temperature near the superconducting transition. The dashed line is the GL mean-field prediction.

where N_0 and γ are nonuniversal parameters related to the vortex-core energy. Above T_c, the theoretical prescription $y(l_+,\tilde{T})=y(0,\tilde{T})$ for truncating the renormalization process introduces a new length scale, the correlation length $\xi_+(\tilde{T})\equiv ae^{l_+(\tilde{T})}$ which measures the average distance between free vortices.

Unlike vortex excitations in ideal superconducting films, vortices in networks experience the pinning effect due to the underlying periodic structure. Using a continued-fraction method, it is possible to estimate the ac vortex mobility in networks by studying the Brownian motion of an individual vortex exposed, for simplicity, to a sinusoidal force field.[14] At the low frequencies used in our experiments, the result is

$$\mu(T)=(a/\phi_0)^2R(T)=(a/\phi_0)^2R_s[I_0(U/2k_BT)]^{-2},$$

where $I_0(x)$ is the modified Bessel function of order zero and U the potential barrier created by the interconnecting links. To estimate the activation energy, we observe that in the critical region the strip width is such that $w/\xi\gg 1$ [typically, $w/\xi(T_\omega)\approx 10$], thereby requiring the nucleation of a normal vortex core during the link crossing process.[15] Thus, U will be almost entirely determined by the condensation energy associated with the core nucleation process. Using Clem's vortex model,[16] we find $U/2k_BT\approx(\pi a/4w)\tilde{T}^{-1}$. In our networks the a/w ratio is so large ($a/w\approx 10$) that, because of the exponential character of $I_0(x)$ for $x\gg 1$, $\mu(T)$ drops by several orders of magnitude in a narrow temperature range below T_{co}, thereby causing the drastic reduction of l_ω which accounts for the observed broadening of the transition. At sufficiently low temperatures, however, vortex pinning and vortex-vortex correlations become so strong that a model based on the Brownian motion of a single vortex excitation is no longer appropriate and the theory is expected to fail. A manifestation of this failure is the "reentrant" behavior of Re[$G(T)$] (not shown in Fig. 2) predicted by the model below a certain temperature $T^*<T_\omega$ ($T^*\approx 2.15$ K in Fig. 2). The origin of this unphysical feature can be traced back to the very short length scales entering renormalization for $T<T^*$. This suggests interpreting the characteristic length at T^*, $r_\omega(T^*)$, as the shortest length scale consistent with the model. Accordingly, in the calculations presented below, $l_\omega(T)$ was kept fixed at $l_\omega(T^*)$ for $T<T^*$ [$l_\omega(T^*)\approx 0.8$ in Fig. 2].

Setting $U/2k_BT\approx a\tilde{T}^{-1}$, the ac conductance data of Fig. 2 were fitted to Eq. (1) using N_0, a, γ, and T_{co} as adjustable parameters (R_s was kept at 750 Ω). An excellent fit of the inductive component is obtained for $N_0=0.18$, $2\pi\gamma=0.82$, $a=7.85$, and $T_{co}=2.258$ K, while the computed dissipative component sets in at temperatures too low to agree with the data. However, considering the high sensitivity of the response to vortex pinning and the approximate method used to incorporate its effect in the dynamical theory, we feel that dissipation is, on the whole, remarkably well described by our model. The value of a is in very good agreement with the predition of Clem's model, whereas T_{co} is consistent with the result extracted from the paraconductivity contribution to the dc conductance above T_{co}. Using a and T_{co} as deduced from the fit, we can estimate the typical length scales explored at 65 kHz: we find $l_\omega=1.13$ ($r_\omega=3.1a$) at $T_\omega=2.166$ K. From the expression relating N_0 and γ to the vortex dielectric constant ϵ_c (Ref. 9) we find $\epsilon_c=1.67$, a value in good agreement with the result ($\epsilon_c\approx 1.70$) of Monte Carlo simulations.[17] Finally, from the universal prediction $K^{-1}(\infty,\tilde{T}_c)=\epsilon_c\tilde{T}_c=\pi/2$ we obtain $T_c=2.146$ K.

As demonstrated by the data of Fig. 1 and predicted by the dynamical theory, the vortex unbinding transition shifts to higher temperatures with increasing ω. If one identifies T_ω as the temperature where the crossover from a vortex-pair- to a free-vortex-dominated response occurs, then T_ω is implicitly defined by $r_\omega(\tilde{T}_\omega)\approx\xi_+(\tilde{T}_\omega)$.[5] To test this fundamental prediction, $r_\omega(\tilde{T}_\omega)$ was deduced from the measured T_ω, while $\xi_+(\tilde{T})$ was computed from the theoretical prescription $y(l_+,\tilde{T})=y(0,\tilde{T})$. All calculations were consistently performed with the parameter values which fit the data of Fig. 2. The results, expressed in terms of the dimensionless quantities l_ω^{-2} and l_+^{-2}, are shown in Fig. 3 as a function of the reduced-temperature shift $(\tilde{T}_\omega-\tilde{T}_c)$. For small shifts (low ω) the scaling parameter inferred from experiment (l_ω) is in excellent agreement with theory (l_+), whereas deviations from the predicted behavior occur for large shifts of T_ω (high ω). This might be due to the fact that the KT theory is less accurate at temperatures well above T_c. Figure 3 also shows that the large length scales required to explore the region very close to T_c were not accessible in our experiments. In this temperature range $l_+^{-2}(\tilde{T})$ is predicted[4,13] to assume the asymptotic form $l_+^{-2}=b(\tilde{T}-\tilde{T}_c)$. If b is consistently computed[9] from N_0 and ϵ_c ($b=0.51$), the data cannot be fitted by this expression, which is obeyed only in a very narrow (~2 mK) interval just above T_c. In light of this result, evidence for the square-root singularity of $l_+(\tilde{T})$ found in previous work[9,10] should be reconsidered.

In conclusion, measurements of the complex ac conductance of weakly coupled superconducting wire networks

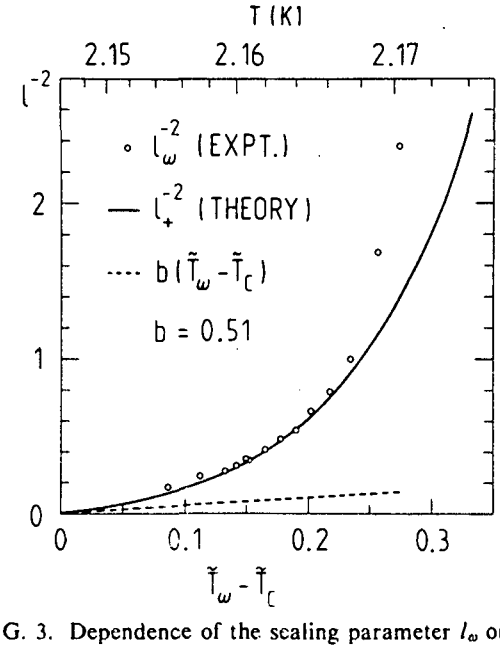

FIG. 3. Dependence of the scaling parameter l_ω on the shift of the dimensionless vortex-unbinding temperature $\tilde{T}_\omega$. The solid line is the prediction of the dynamical KT theory, the dashed line its asymptotic form very close to T_c.

have provided the first observation of the Kosterlitz-Thouless vortex unbinding transition in this system. The remarkable degree of quantitative agreement emerging from the theoretical analysis of the dynamic response suggests that weakly coupled wire networks will also be ideal model systems for studies of critical phenomena in frustrated and/or disordered two-dimensional systems. Apart from their intrinsic fundamental importance, such investigations should provide a deeper understanding of some of the intriguing magnetic properties of high-temperature superconducting ceramics.

We would like to thank H. Beck for many stimulating discussions and U. Mohr, D. Varidel, and Y. Oppliger for technical assistance. This work was supported by the Swiss National Science Foundation.

[1]For a recent review of the field, see *Coherence in Superconducting Networks*, edited by J. M. Mooij and G. B. J. Schön [Physica B **152**, Nos. 1 and 2 (1988)].

[2]B. Pannetier, J. Chaussy, R. Rammal, and J. C. Villegier, Phys. Rev. Lett. **53**, 1845 (1984).

[3]A. T. Fiory and A. F. Hebard, in *Inhomogeneous Superconductors—1979*, edited by D. U. Gubser, T. L. Francavilla, S. A. Wolf, and J. R. Leibowitz, AIP Conf. Proc. No. 58 (American Institute of Physics, New York, 1979), p. 293; A. T. Fiory, A. F. Hebard, P. M. Mankiewich, and R. E. Howard, Appl. Phys. Lett. **52**, 2165 (1988); B. Jeanneret, J. L. Gavilano, G. A. Racine, Ch. Leemann, and P. Martinoli, Appl. Phys. Lett. (to be published).

[4]J. M. Kosterlitz and D. J. Thouless, J. Phys. C **6**, 1181 (1973).

[5]V. Ambegaokar, B. I. Halperin, D. R. Nelson, and E. D. Siggia, Phys. Rev. B **21**, 1806 (1980); S. R. Shenoy, J. Phys. C **18**, 5163 (1985).

[6]D. J. Bishop and J. D. Reppy, Phys. Rev. B **22**, 5171 (1980).

[7]A. T. Fiory, A. F. Hebard, and W. I. Glaberson, Phys. Rev. B **28**, 5075 (1983).

[8]S. Teitel and C. Jayaprakash, J. Phys. (Paris) Lett. **46**, L33 (1985).

[9]J. E. Mooij, in *Percolation, Localization and Superconductivity*, edited by A. M. Goldman and S. A. Wolf (Plenum, New York, 1984), p. 325.

[10]Ch. Leemann, Ph. Lerch, G.-A. Racine, and P. Martinoli, Phys. Rev. Lett. **56**, 1291 (1986).

[11]A. T. Fiory, A. F. Hebard, P. M. Mankiewich, and R. E. Howard, Phys. Rev. Lett. **61**, 1419 (1988).

[12]L. G. Aslamasov and A. I. Larkin, Fiz. Tverd. Tela. **10**, 1104 (1968) [Sov. Phys. Solid State **10**, 875 (1968)].

[13]J. M. Kosterlitz, J. Phys. C **7**, 1046 (1974).

[14]P. Martinoli, M. Nsabimana, G.-A. Racine, H. Beck, and J. R. Clem, Helv. Phys. Acta **56**, 765 (1983).

[15]K. K. Likharev, Rev. Mod. Phys. **51**, 101 (1979).

[16]J. R. Clem, J. Low Temp. Phys. **18**, 427 (1975).

[17]S. Teitel and C. Jayaprakash, Phys. Rev. B **27**, 598 (1983).

DYNAMICAL STUDY OF THE SUPERCONDUCTING PHASE TRANSITION OF TWO-DIMENSIONAL NETWORKS

B. Jeanneret, Ph. Flückiger, Ch. Leemann and P. Martinoli
Institut de Physique, Université de Neuchâtel, 2000 Neuchâtel, Switzerland

Abstract

Granular aluminum wire networks forming square arrays of N x N = 10^6 nodes connected by strips 8 μm long were fabricated with photolithographic techniques. For strip resistances of the order of 1kΩ the superconducting transition of the network, as evidenced by ac conductance measurements, is shown to be of the Kosterlitz-Thouless type. In a perpendicular magnetic field, flux quantization in the loops of the network leads to periodic oscillations of the magnetoconductance.

1. Introduction

Josephson junction arrays and superconducting wire networks[1] provide excellent model systems to study composite materials where superconducting grains or clusters embedded in a non-superconducting matrix are coupled together by the Josephson effect. The situation is comparable to the one encountered in the study of high temperature superconducting ceramics. When compared to granular materials, however, artificial networks offer considerable advantages : their topology, as well as their relevant physical parameters, can be accurately controlled and selected to explore a few specific aspects of an otherwise complex problem.

In this paper we focus our attention on the critical behavior of periodic wire networks. The nature of the superconducting-to-normal transition of wire networks is determined by the ratio a/ξ between the lattice spacing a and the Ginzburg-Landau (GL) coherence length ξ. For a ≪ ξ the Josephson coupling energy dominates the condensation energy[2] and, as a consequence, adjacent nodes of the network are strongly coupled to each other. In this case thermal fluctuations in the phase of the complex order parameter at the nodal sites are irrelevant and the phase boundary in the (H,T) plane is obtained by solving a linearized GL equation[3,4]. This strong coupling regime has been extensively investigated by Pannetier and coworkers[5]. The mean field GL approach, however, is no longer valid in the weak coupling limit (a ≫ ξ), where two-dimensional (2D) phase fluctuations create vortex excitations which are essential in determining the critical behavior of a wire network. According to the Kosterlitz-Thouless (KT) theory[6], applicable to the a ≫ ξ case, the transition to the resistive state in zero magnetic field is triggered by the unbinding of vortex pairs and is predicted to occur at a temperature T_c lower than the mean field critical temperature T_{co}. While a vortex unbinding transition has been clearly observed in proximity effect and tunnel junction arrays[1,7,8], for wire networks only limited evidence for KT critical behavior exists[9].

In the following we report a study of the complex ac conductance G of square networks of granular aluminum wires in the critical region. In zero magnetic field the ac response of weakly coupled networks shows, below T_{co}, features which strongly support the existence of a phase transition with KT character. Measurements of the oscillatory ac magnetoconductance of moderately coupled networks are also presented and briefly discussed.

2. Sample Fabrication

Granular aluminum films were evaporated onto silicon wafers held at room temperature. The film thickness d (between 200 Å and 700 Å) and the deposition rate were measured in situ with a standard quartz thickness monitor. The desired resistivity was achieved by carefully adjusting the deposition rate and the partial pressure of oxygen during the evaporation[10]. The samples were then patterned photolithographically, by contact printing a mask produced by electron beam lithography. The final result, shown in Fig. 1, is a network of aluminum wires of width w = 1 μm, forming a square lattice of N x N = 10^6 nodes with lattice parameter a = 8 μm and strip resistance R_s ranging from 10 Ω to 1 kΩ.

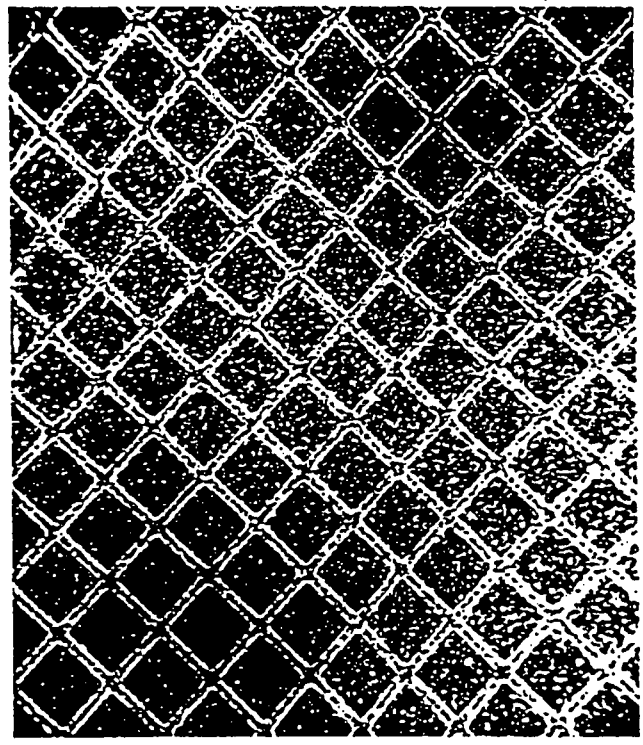

Figure 1. Scanning electron micrograph of an aluminum wire network. The lattice parameter is a = 8 μm.

Since the Josephson coupling energy E_J is proportional to i_c, the critical current of a strip, which in turn is proportional to R_s^{-1} [11], it is possible to cover a wide range of coupling strengths by varying R_s. We found that strip resistances of the order of a few Ohms result in strongly coupled networks with mean field-like behavior. As R_s increases, the nodes slowly decouple, the weak coupling limit being reached when $R_s \sim 1$ kΩ.

Manuscript received August 22, 1988

3. Conductance Measurements

At temperatures below T_{co} the sheet impedance Z of the network is weak. A measuring method which couples directely to the sheet conductance presents therefore a largely increased sensitivity compared to resistive measurements, allowing to test the vortex unbinding mechanism predicted by the KT theory.

The complex conductance $G = Z^{-1}$ of the networks was measured with a mutual inductance detector[11,12] consisting of a cylindrical drive coil and an internal concentric pair of astatic detection coils. A current I_D of angular frequency ω flowing in the excitation coil will induce screening currents in the network which in turn will induce an out-of-balance signal δV in the detection coils. In the weak screening limit[1] this signal is given by

$$\delta V = C\,\omega^2 I_D\, G(\omega,T) \qquad (1)$$

where C is a constant depending of the geometrical parameters of the detector.

At low temperatures, but still in the GL regime, the following mean field behavior is expected :

$$\mathrm{Re}(G) = 0 \qquad (2)$$

$$\mathrm{Im}(G) = \frac{1}{\omega L_k} \qquad (3)$$

where $L_k \propto R_s/(T_{co}-T)$ [9] is the kinetic inductance. In Fig. 2, the real and imaginary parts of the conductance as well as the resistive transition are presented for a weakly coupled network. At low temperatures $\mathrm{Im}(\delta V)$ decreases linearly and $\mathrm{Re}(\delta V) = 0$ as predicted by equation (2) and (3). In the vicinity of the transition however, a dramatic deviation from the mean field prediction occurs. A jump in $\mathrm{Im}(\delta V)$ and a peak in $\mathrm{Re}(\delta V)$ appear in a narrow temperature range below T_{co}. This renormalisation of the conductance is due to vortex excitations predicted by the KT theory, showing that the phase transition is triggered by fluctuations in the phase of the complex order parameter[7].

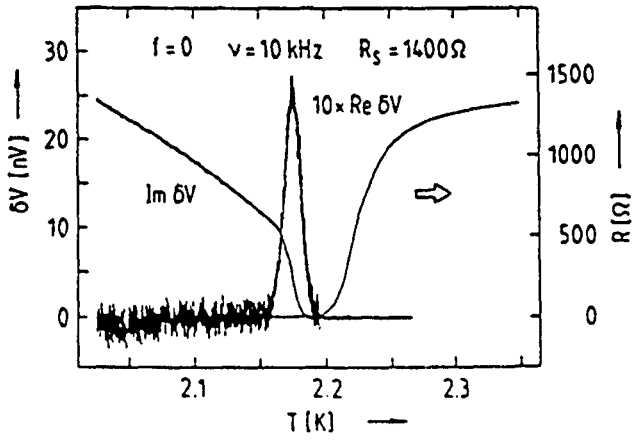

Figure 2. Real and imaginary parts of the conductance of a weakly coupled network, as well as its dc resistance, as a function of temperature.

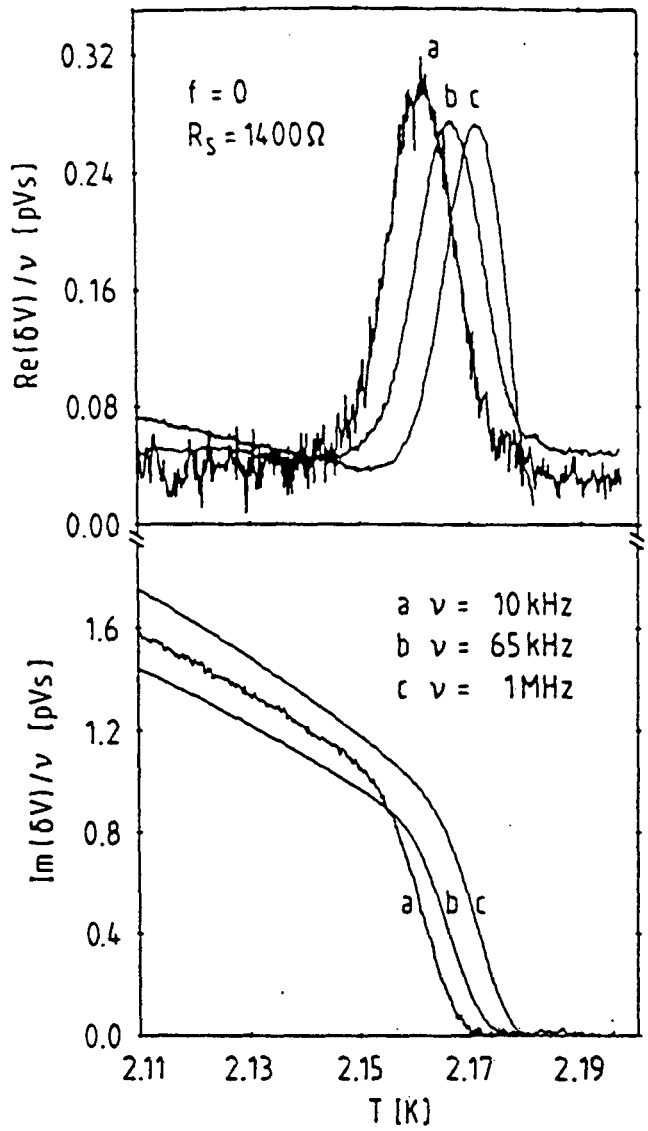

Figure 3. Real and imaginary parts of the ac conductance as a function of temperature at three different frequencies.

With the low temperature linear part of $\mathrm{Im}(\delta V)$ of Fig. 2, we can determine the constant C of equation (1). We find $C = 6.8 \cdot 10^{-17} V^2 s^2/A^2$, in good agreement with the value obtained with a numerical calculation based on the geometrical parameters of the detector. Defining T_c as the temperature corresponding to the break in $\mathrm{Im}(\delta V)$, ($T_c \approx 2.17K$), the renormalized value of the kinetic inductance, $L_{kR}(T_c)$, inferred from Fig. 2 and equations (1) and (3), leads to $L_{kR}T_c = 1.32 \cdot 10^{-8} HK$, close to the universal KT prediction $L_{kR}T_c = 1.23 \cdot 10^{-8} HK$ [13]. A more detailed analysis of these data will be published elsewhere.

In Fig. 3 experimental curves of the ac response at different frequencies show that the transition temperature is frequency dependent, as expected in a dynamical extension of the KT theory[14]. At the transition temperature T_c vortex-antivortex pairs of infinite size unbind, as the temperature increases beyond T_c, pairs of successively smaller size unbind. At nonzero measuring frequencies only pairs of size smaller than the probing length r_ω contribute to the response[14]. Since r_ω decreases with frequen-

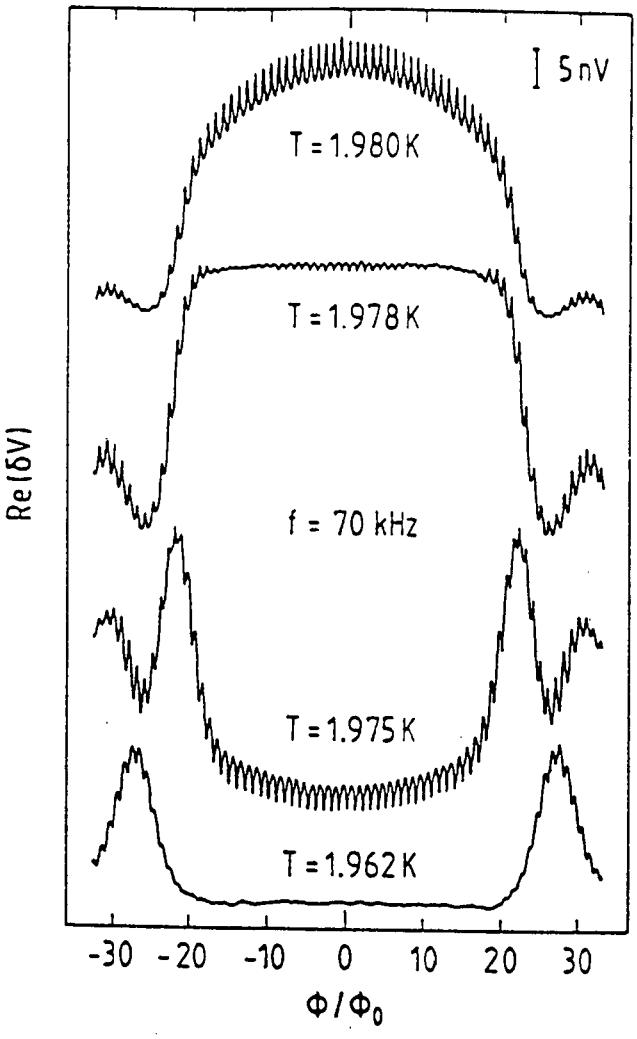

Figure 4a. Real part of the magnetoconductance for a sample with $R_s \approx 10^2\Omega$ at four different temperatures.

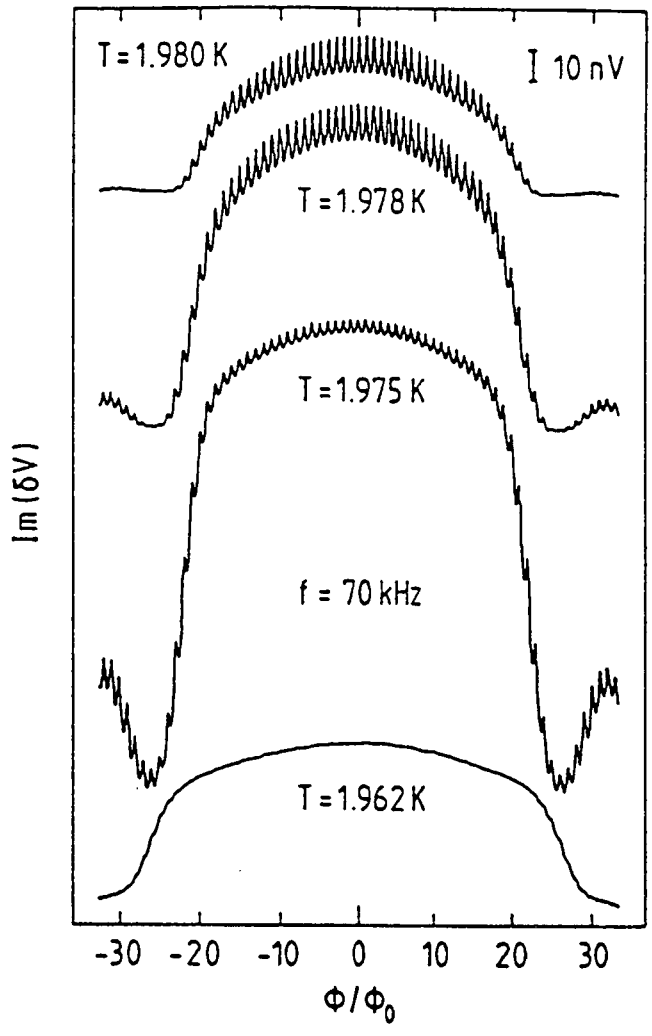

Figure 4b. Imaginary part of the magnetoconductance for a sample with $R_s \approx 10^2\Omega$ at four different temperatures.

cy, the transition temperature is observed at higher temperatures as the frequency is increased, in accordance with the measurements reported in Fig. 3.

4. Magnetic Field Effects

In a perpendicular magnetic field a regular network in the transition region is uniformly frustrated with a frustration parameter f given by the applied magnetic flux per unit cell in units of the superconducting flux quantum[1]. The real and imaginary parts of the ac conductance as a function of f at four different temperatures is shown in Fig. 4, for a sample with $R_s \approx 10^2$ Ω. In a small temperature range below T_{co} both components of δV show oscillations of period unity persisting out to $f \sim 40$, indicating a high degree of sample uniformity. In lower resistance samples structures at small half integer f-values have also been observed[9]. The complexity of the envelope of the signals of Fig. 4 is at present not well understood in every detail. Its main features, however, can be qualitatively understood by taking into account two effects : the reduction of the mean field transition temperature due to the magnetic field, and a diffraction-like modulation due to the dependence of i_c on B in a single strip.

As an example of the effect of the magnetic field onto T_{co}, consider the T = 1.975 K curve of Fig. 4a: at low magnetic fields, flux quantization in the unit cells dominates and the signal returns to its f = 0 value every Δf = ±1. Gradually, however, the magnetic field lowers T_{co}; as a result, while at f = 0 we were to the left of the peak of Fig. 2, at $f \sim 20$ the signal has reached its peak value, and then slowly decreases again.

The diffraction-like pattern is most easily observed in the T = 1.975 K curve of Fig. 4b where the minimum at $f \approx 27$ is believed to correspond to one flux quantum in each strip. This interpretation is supported by two observations : the applied magnetic field corresponds to one flux quantum in an area of the order of $\omega\xi(T)$ and the minimum shifts to higher field values as the temperature is lowered, in accordance with the temperature dependence of $\xi(T)$.

5. Conclusions

The unique features of the dynamics of vortex excitations can be most sensitively probed with an experimental method measuring directly the sheet conductance of the samples.

The properties of regular wire networks, as investigated with ac conductance measurements, show that the KT transition can indeed be observed in weakly coupled samples. The temperature dependence and, albeit only qualitatively, the frequency dependence of their ac response presented here are in agreement with a description of the critical behavior in terms of the KT vortex unbinding mechanism.

Dr. J. Beguin's scanning electron micrograph, useful discussions with Dr. J.L. Cavilano and technical assistance by U. Mohr are gratefully acknowledged. This work was supported by the Fonds National Suisse pour la Recherche Scientifique.

References

[1] P. Martinoli, Ph. Lerch, Ch. Leemann, and H. Beck, "Arrays of Josephson Junctions.: Model systems for Two-Dimensional Physics", Jpn. J. Appl. Phys., vol. 26-3, p. 1999, 1987.

[2] J. R. Clem, "Granular and superconducting-glass properties of the high-temperature superconductors", Physica C, vol. 153-155, p. 50, 1988.

[3] S. Alexander and E. Halevi, "Superconductivity on networks : II. The London approach", J. Physique, vol. 44, p. 805, 1983.

[4] S. Teitel and C. Jayaprakash, "Resistive transitions in regular superconducting wire networks", J. Physique Lett., vol. 46, p. L33, 1985.

[5] B. Pannetier, J. Chaussy and R. Rammal, "Experimental Fine Tuning of Frustration : Two-Dimensional Superconducting Network in a Magnetic Field", Phys. Rev. Lett., vol. 53, p. 1845, 1984.

[6] J. M. Kosterlitz and D. J. Thouless, "Ordering, metastability and phase transitions in two-dimensional systems", J. Phys. C, vol. 6, p. 1181, 1973.

[7] Ch. Leemann, Ph. Lerch, G.-A. Racine and P. Martinoli, "Vortex Dynamics and Phase Transitions in a Two-Dimensional Array of Josephson Junctions", Phys. Rev. Lett., vol. 56, p. 1291, 1986.

[8] B. J. van Wees, H. S. van der Zant and J.E. Mooij, "Phase transitions of Josephson-tunnel-junction arrays at zero and full frustration", Phys. Rev. B, vol. 35, p. 7291, 1987.

[9] B. Jeanneret, Ch. Leemann and P. Martinoli, "Dynamics of the Phase Transition of Periodic Superconducting Networks", Jpn. J. Appl. Phys., vol. 26-3, p. 1417, 1987.

[10] G. Deutscher, H. Fenichel, M. Gershenson, E. Grünbaum and Z. Ovadyahu,"Transition to Zero Dimensionality in Granular Aluminum Superconducting Films", J. Low. Temp. Phys., vol. 10, p. 231, 1973.

[11] V. Ambegaokar and A. Baratoff, "Tunneling between superconductors", Phys. Rev. Lett., vol. 10, p. 486, 1963.

[12] A. F. Hebard and A. T. Fiory, "Evidence for the Kosterlitz-Thouless Transition in Thin Superconducting Aluminum Films", Phys. Rev. Lett., vol. 44, p. 291, 1980.

[13] C. J. Lobb, D. W. Abraham and M. Tinkham, "Theoretical interpretation of the resistive transition data from arrays of superconducting weak links", Phys. Rev. B, vol. 27, p. 150, 1983.

[14] V. Ambegaokar, B. I. Halperin, D. R. Nelson, and E. D. Siggia, "Dissipation in Two-Dimensional Superfluids", Phys. Rev. Lett., vol. 40, p. 783, 1978.

COMPLEX AC CONDUCTANCE OF YBaCuO FILMS

P.K. Srivastava[1], P. Oebély[1], H.E. Hintermann[1],
Ch. Leemann[2], Ph. Flückiger[2], O. Caccivio[2], J.-L. Cavilano[2], J. Weber[2] and P. Martinoli[2],
[1] CSEM, 2000 Neuchâtel, Switzerland
[2] Institut de Physique, Université de Neuchâtel, 2000 Neuchâtel, Switzerland

Abstract

The ac linear response of YBaCuO films prepared by RF magnetron sputtering to a small oscillating field was studied as a function of temperature and transverse magnetic field. The results are interpreted within the framework of a Josephson junction network model for the films, with the grain boundaries acting as the junctions.

1. Introduction

The relatively low critical currents in high temperature superconducting ceramics[1], are believed to be a result of Josephson weak link effects within the material itself. The actual location of the weak links is still uncertain. While intuitively one would expect the grain boundaries to play the role of Josephson junctions[2,3], it has also been suggested[4-6] that the junctions are located within the physical grains of the ceramic. In this latter model the superconducting islands are distributed on weakly site disordered two dimensional (2D) lattices where the islands of orthorhombic phase are Josephson coupled through a non superconducting host - the tetragonal phase. In the present paper we report an investigation of the superconducting transition of YBaCuO films with a two coil mutual inductance technique[7]. This method allows a direct measurement of the complex ac conductance of thin films, proportional to the inverse superfluid kinetic inductance L_k, which in turn is proportional, in Josephson junction arrays, to the helicity modulus[8-10]. It should be emphasized that this type of measurement, very sensitive in the sample's superconducting state, is much more apt to probe array-like properties than dc resistive measurements.

We find that in superconducting YBaCuO films the temperature dependence of the ac conductance is qualitatively identical to that observed in artificially prepared 2D Josephson junction networks[9,11]. In a perpendicular magnetic field the conductance exhibits irregular but, within one thermal cycle, reproducible oscillations, similar to those observed in bulk magnetoresistance measurements[12], and reminescent of flux quantization effects in periodic arrays[9,13].

2. Sample Preparation and Characterization

RF magnetron sputtering from a ceramic $YBa_2Cu_3O_7$ target was used for the deposition of superconducting oxide films. The targets were fabricated by mixing the proper amounts of Y_2O_3, $BaCO_3$ and CuO powders, sintering at 950 C for 48 hours in an oxygen atmosphere, regrinding and pressing the powders into 75 mm diameter and 3 mm thick discs and annealing these discs at 950 C for 10 hours in an oxygen atmosphere. The targets thus prepared were superconducting with a transition onset at 94 K and zero resistance at 92 K. The films, typically 3 μm thick, were deposited on sapphire substrates held at 300 C. An Argon - Oxygen (up to 20 %) gas mixture was used as sputtering gas and the sputtering was carried out at a pressure of 4 Pa. The distance between target and substrate was 40 mm. The RF power applied was of the order of 5 W/cm^2. Under these conditions a deposition rate of ~ 60 Å/min. was obtained. The films, as deposited, were electrically insulating. They were annealed at 920 C for 5 min. in an oxygen atmosphere. By optimizing heating and cooling rates, superconducting films were obtained. Electron microprobe and Rutherford backscattering (RBS) techniques were used to determine the composition of the films. It was observed that the composition of the films can be varied to a large extent by varying the target to substrate distance and by varying the position of the substrates beneath the magnetron erosion zone. The films which were deposited in the center of the magnetron erosion zone and at a target to substrate distance of 40 mm had an Y:Ba:Cu ratio of 1:2:3 whereas others had an excess of Yttrium. It was also found that the amount of oxygen in the film could be fine tuned to its proper value by controlling the heating and the cooling rates. The result of an RBS measurement is shown in figure 1. It was found that on the film surface (right flank of the graph) the Y:Ba:Cu ratios were, within the experimental accuracy of the method, the correct 1:2:3 stoichiometry. On the other hand, at the interface with the sapphire substrate (left flank of the graph), the step like structure is washed out - an indication of an interdiffusion process of the sapphire and film material[14].

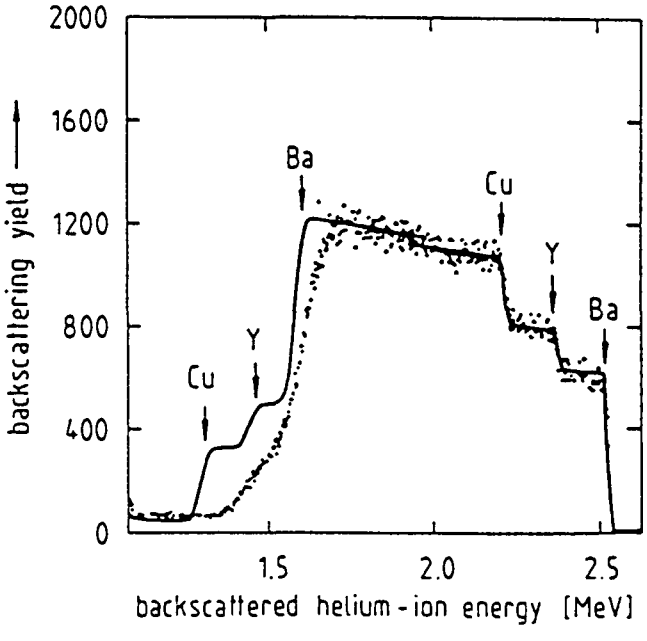

Figure 1. RBS spectrum of a relatively thin (1.5 μm) YBaCuO film. Points : measured spectrum; full line : calculated spectrum for a 1:2:3:7 stoichiometry. The discrepancy at the left flank indicates interdiffusion of the YBaCuO with the sapphire substrate.

Manuscript received August 22, 1988

3. Experimental Results

The superconducting transitions, as seen in dc resistive measurements, of three films, YBCO1, YBCO2 and YBCO3 are shown in figure 2. Both YBCO1 and YBCO2 have a transition midpoint at T_{co} = 90 K. Notice however that, while YBCO1 is metallic in the normal state and has a sharp transition, YBCO2 has a slightly negative dR/dT above the transition and has a long resistive tail extending down to about 75 K. YBCO3 on the other hand shows clear semiconductor-like behavior, with a dc superconducting transition setting in only below 40 K. These observations, typical for granular superconductors[15], are interpreted in terms of different strengths of Josephson coupling energies between the superconducting clusters in the various films.

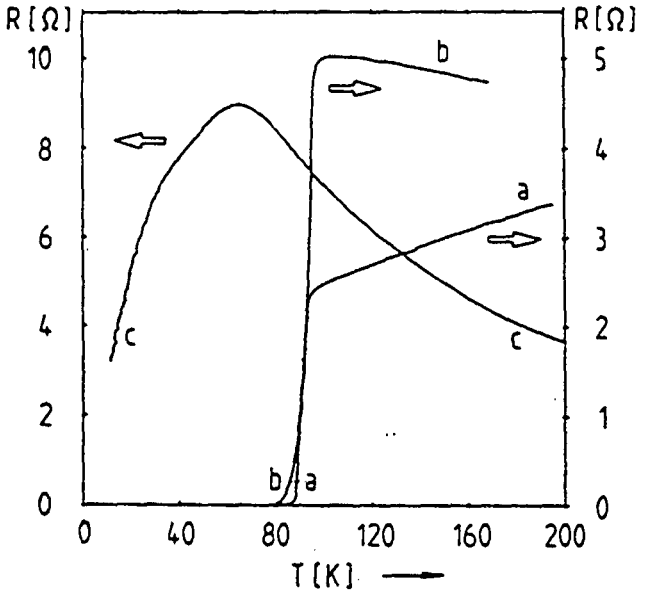

Figure 2. Temperature dependence of the dc resistance of the three YBaCuO films a,b and c corresponding, respectively, to YBCO1, YBCO2 and YBCO3.

In order to investigate the complex ac conductance of the YBCO films, we have used a two coil mutual inductance technique described elsewhere[7-9,16]. Figures 3 and 4 show the temperature dependence of the

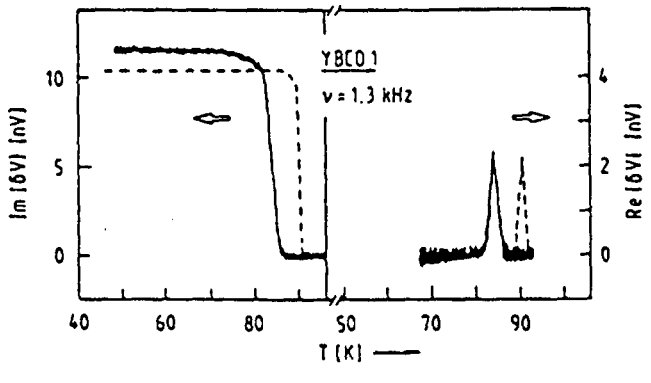

Figure 3. Full line : temperature dependence of the complex ac response of the YBCO1 film, relatively thick (~ 5 μm). Dashed line : the same measurement for a bulk sample.

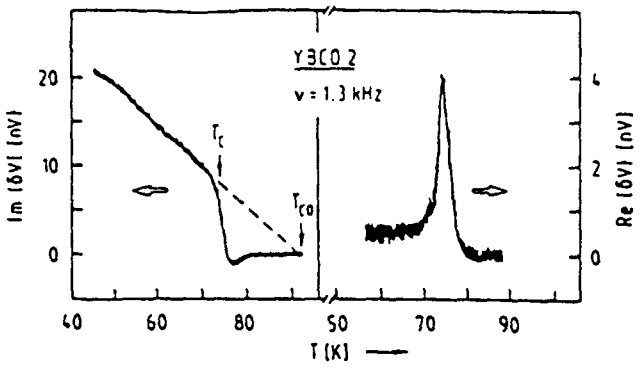

Figure 4. Temperature dependence of the complex ac response of sample YBCO2.

complex ac response of the two samples YBCO1 and YBCO2, respectively. The ac response of YBCO1 is, except for a small (~ 7 K) shift to lower temperatures and a small amount of broadening, identical to that of a bulk sample, characterized by strong screening. As already suggested by the dc measurement, YBCO2 is modeled as a network of weakly coupled Josephson tunnel junctions, with a Josephson penetration depth large compared to the film thickness. Then the weak screening limit is applicable and the signal voltage at the gradiometer detection coil can be expressed in the following way[9] :

$$\delta V = C.\omega^2.I_D.G(\omega,T)$$

where I_D is the amplitude of the current of angular frequency ω flowing in the excitation coils, G is the sheet conductance of the film and C a constant depending on the sample-coil geometry. If the dissipative contribution to the conductance is negligible, $G = (i\omega L_k)^{-1} \propto i_c(T)$, the critical current of a single junction. We thus expect, using the Ambegaokar - Baratoff expression for the critical current of tunnel junctions[17], $Im(\delta V) \propto (T_{co}-T)$ at not too low temperatures. This linear temperature dependence is evident in figure 4, also notice that Im(δV) extrapolates to zero at the bulk transition temperature T_{cb} = 92K. The most exciting aspects of figure 4 however, are the sudden drop of the superfluid component, Im(δV), at a temperature T_c ~ 75 K and its similarity to the behavior observed in 2D periodic junction arrays[8,9,11] where the superconducting transition is governed by the vortex unbinding mechanism of the Kosterlitz - Thouless theory[18]. A detailed discussion of the applicability of the vortex unbinding idea to the superconducting transition of YBaCuO films will be presented elsewhere[19].

The Josephson-array interpretation of our films is further supported by measurements of the ac conductance in a perpendicular magnetic field. As evidenced by figure 5, in the transition region the magnetoconductance exhibits oscillations which are irregular but, at least within one thermal cycle, reproducible. These structures are thought to arise from quantum interference effects in superconducting loops, an interpretation supported by a Fourier analysis of the data of figure 5, shown in figure 6 and yielding (1-4) μm for the typical loop size, of the order of the grain size. Magnetoconductance oscillations are expected to occur in small size granular samples (up to 100 grains)[2] or in regular arrays[9]. It is thus very surprising that such oscillations appear in our measurements; we estimate the area under the detection coils to be occupied by some 10^5 grains !

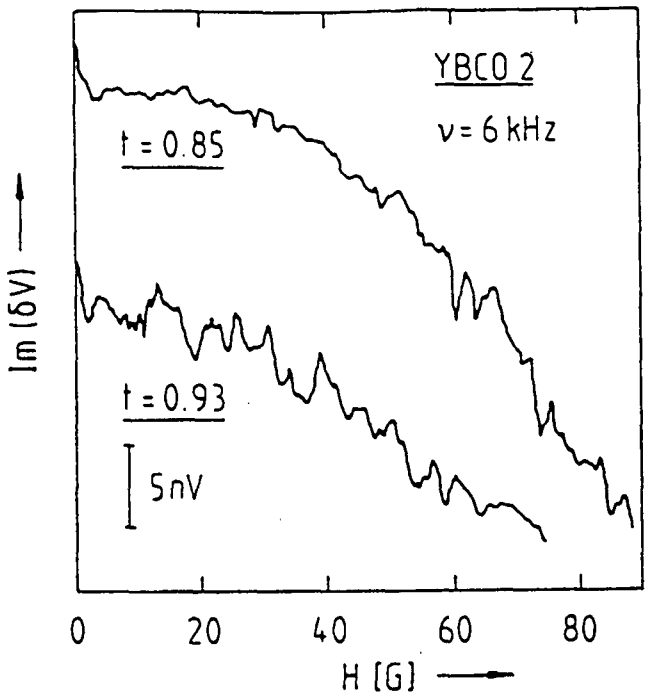

Figure 5. Magnetic field dependence of Im(δV) of the YBCO2 film at two different reduced temperatures $T \equiv T/T_{co}$. The oscillations, though irregular, are reproducible and disappear below the transition region.

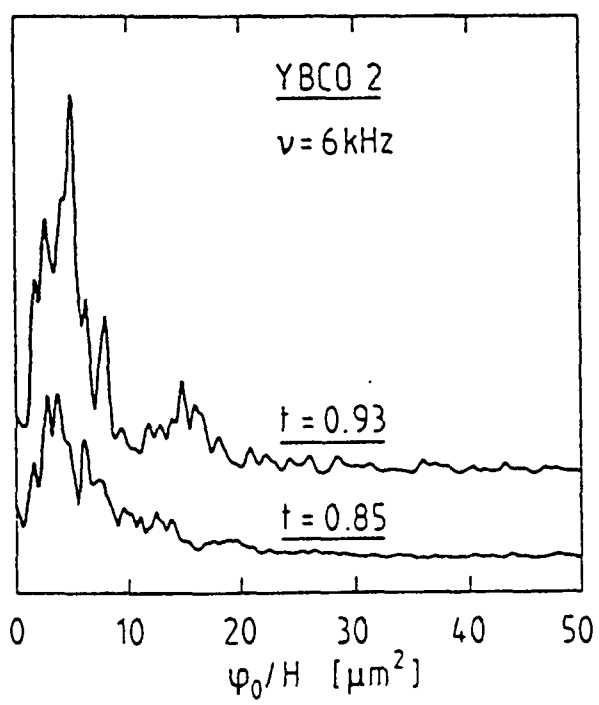

Figure 6. Magnitude of the fast Fourier transform of the two curves of figure 5, showing that the loop area relevant for flux quantization effects is of the order of a few μm^2.

4. Conclusions

The structures observed in the ac response of thin $YBa_2Cu_3O_7$ films are quite similar to those found in artificially prepared 2D periodic junction arrays[9,10,15], where the transition from a phase ordered to a phase disordered state et T_c is attributed to the vortex unbinding mechanism predicted by the Kosterlitz-Thouless theory[18] for phase transitions in two dimensions. The magnetic field data suggest that the typical cell size of the YBCO "array" is a few μm, of the order of the grain size. We are led to believe that our ceramic films can be modeled as 2D networks of Josephson tunnel junctions, the junctions being located at the grain boundaries.

Our work was supported by the Swiss National Science Foundation.

References

[1] J.G. Bednorz and K.A. Müller, "Possible High T_c Superconductivity in the Ba-La-Cu-O System", Z. Phys. B64, 189, 1986.

[2] C. Ebner and D. Stroud, "Diamagnetic Susceptibility of Superconducting Clusters : Spin-Glass Behavior", Phys. Rev. B31, 165, 1985.

[3] S. John and T.C. Lubensky, "Phase Transitions in a Disordered Granular Superconductor Near Percolation", Phys. Rev. B34, 4815,1986.

[4] G. Deutscher and K.A. Müller, "Origin of Superconductive Glassy State and Extrinsic Critical Currents in High-T_c Oxides", Phys. Rev. Lett. 59, 1745, 1987.

[5] I. Morgenstern, K.A. Müller and J.G. Bednorz, "Numerical Simulations of a High-T_c Superconductive Glass Model", Z. Phys. B69, 33, 1987.

[6] K.A. Müller, M. Takashige and J.G. Bednorz, "Flux Trapping and Superconductive Glass State in La_2CuO_{4-y}:Ba", Phys. Rev. Lett. 58, 1143, 1987.

[7] A.F. Hebard and A.T. Fiory, "Vortex Dynamics in Two-Dimensional Superconductors", Physica (Amsterdam) 109&110 B+C, 1637, 1982, and "Penetration Depths of High T_c Films Measured by Two-Coil Mutual Inductances", Aopl. Phys. Lett. 52, 2165, 1988.

[8] Ch. Leemann, Ph. Lerch, G.-A. Racine and P. Martinoli, "Vortex Dynamics and Phase Transitions in a Two-Dimensional Array of Josephson Junctions", Phys. Rev. Lett. 56, 1291, 1986.

[9] P. Martinoli, Ph. Lerch, Ch. Leemann and H. Beck, "Arrays of Josephson Junctions : Model Systems for Two-Oimensional Physics", Jpn. J. Appl. Phys. 26, Suppl. 26-3, 1999, 1987.

[10] C. Ebner and D. Stroud, "Superfluid Density, Penetration Depth, and Integreted Fluctuation Conductivity of a Model Granular Superconductor", Phys. Rev. B28, 5053, 1983.

[11] B. Jeanneret, Ch. Leemann and P. Martinoli, "Dynamics of the Phase Transition of Periodic Superconducting Networks", Jpn. J. Appl. Phys. 26, Suppl. 26-3, 1417, 1987.

[12] R. Steinmann, P. Lejay, J. Chaussy and B. Pannetier, "Magnetoresistance Oscillations in Bulk High T_c Superconductor", Physica 153-155, 1487, 1988.

[13] B. Pannetier, J. Chaussy, R. Rammal and J.C. Villegier, "Experimental Fine Tuning of Frustration : Two-Dimensional Superconducting Network in a Magnetic Field, Phys. Rev. Lett. 53, 1845, 1984.

[14] D. K. Lathrop, S.E. Russek and R.A. Buhrman, "Production of $YBa_2Cu_3O_{7-y}$ Superconducting Thin Films in Situ by High-Pressure Reactive Evaporation and Rapid Thermal Annealing", Appl. Phys. Lett. 51, 1554, 1987.

[15] Y. Shapira and G. Deutscher, "Semiconductor-Superconductor Transition in granular Al-Ge", Phys. Rev. B27, 4463, 1983.

[16] Ch. Leemann, Ph. Lerch, R. Théron and P. Martinoli, "The Kosterlitz-Thouless Transition in Josephson Junction Arrays", Helv. Phys. Acta 60, 128, 1987.

[17] V. Ambegaokar and A. Baratoff, "Tunneling Between Superconductors", Phys. Rev. Lett. 10, 486, 1963.

[18] J.M. Kosterlitz and D.J. Thouless, "Ordering, Metastability and Phase Transitions in Two-Dimensional Systems", J. Phys. C6, 1181, 1973.

[19] P. Martinoli, J. Gavilano and Ph. Flückiger, to be published.

GROWTH OF R.F. MAGNETRON SPUTTERED $Y_1Ba_2Cu_3O_7$ THIN FILMS

P.K. Srivastava*, P. Debély*, H. Boving* and H.E. Hintermann*

Ph. Flückiger°, Ch. Leemann°, J. Weber° and P. Martinoli°

ABSTRACT

R.F. Magnetron sputtering from a ceramic $Y_1Ba_2Cu_3O_7$ target in mixed Ar-O_2 atmosphere followed by O_2 annealing have been used to prepare superconducting oxide films. By optimizing various sputtering parameters and annealing conditions, superconducting transition temperatures at 87K, 88 K and 78 K have been obtained for films deposited on sapphire, polycrystalline ZrO_2-3% Y_2O_3 and monocrystalline MgO (100) substrates respectively. Surface morphology, crystal structure and composition of the films have been characterized by optical microscope using polarized light, scanning electron microscope, X-ray diffraction, electron microprobe analyser and Rutherford backscattering spectroscopy. It is observed that the films are rough and have very large grains in which various twins can be seen. The films, when deposited on MgO substrates, show a preferred grain growth of a superconducting phase with c-axis perpendicular to the film surface whereas films deposited on ZrO_2-3%Y_2O_3 substrates show that a small fraction of randomly oriented superconducting phase is also growing along with the c-axis oriented superconducting phase.

INTRODUCTION

Perovskite type [1] superconducting oxide films ($Y_1Ba_2Cu_3O_{7-x}$)[2] have attracted much interest due to their high potential applications in electronic devices [3] and for fundamental physical studies. Sputtering, being the most common technique for the deposition of films used in electronic devices, has been studied extensively for the deposition of superconducting oxide films. Various type of sputtering processes like, r.f. and d.c. magnetron in pure Ar or Ar-O_2 atmosphere using single [4-8], dual[9, 10] or multiple targets [11-13] have been used to obtain superconducting oxide films. Dual and multiple target sputtering have produced an arrays of films with a phase spread in which few films with composition close to correct stoichiometry do exhibit good superconducting properties, whereas in single target sputtering correct stoichiometric composition can be obtained over large areas by controlling the target composition. These films also show good superconducting properties. Sputtering from a single target has other advantages like easy control of the process parameters and high reproducibility. Keeping these advantages in mind, we have deposited $Y_1Ba_2Cu_3O_7$ films by r.f. magnetron sputtering using a single stoichiometric target followed by annealing under flowing O_2 in a furnace. By optimizing various sputtering parameters and annealing conditions we have obtained superconducting oxide films on sapphire, polycrystalline ZrO_2-3%Y_2O_3 and monocrystalline MgO (100) substrates. Superconducting transition temperatures as determind with a zero d.c. resistance criterium are at 87K, 88K and 78K on sapphire, ZrO_2-3%Y_2O_3 and MgO respectively.

*Swiss Center for Electronics and Microtechnology, Inc., Research and Development, B.P. 41, CH-2007 Neuchâtel, Switzerland
°Institut de Physique, Université de Neuchâtel, CH-2000 Neuchâtel, Switzerland

In our earlier papers [14, 15] we have reported the results of inductive conductance measurements of these films. In this paper we report the morphology, composition, crystal structure and d.c. resistance vs temperature properties of our films.

EXPERIMENTAL DETAILS

R.F. magnetron sputtering from a single stoichiometric target of $Y_1Ba_2Cu_3O_7$ was used for the deposition of superconducting oxide films. The targets (75 mm diameter and 3 mm thick disks) were prepared by a sintering and annealing procedure from powders of yttrium oxide, copper oxide and barium carbonate. Various films with thickness between 0.5 μm to 3.0 μm were deposited on sapphire, ZrO_2-3%Y_2O_3 and MgO(100) substrates held at substrate temperatures ranging between 300 and 400°C. Sputtering was carried out under Ar +20% O_2 atmosphere by keeping the substrate to target distance between 30 and 40 mm. The power applied was 5W/cm^2 and sputtering was done at a pressure of 4Pa. Under these conditions a deposition rate of 60 A°/min. was obtained.

The as deposited films were shiny black and electrically insulating. They were annealed at 920°C for 5 min. in flowing oxygen. During annealing heating and cooling rates were optimized to obtain superconducting oxide films. The as deposited and the annealed films were characterized for surface morphology, composition and crystal structure by optical microscopy using polarized light, scanning electron microscope (SEM), electron microprobe analyser in wavelength dispersive mode (EPMA), Rutherford backscattering spectroscopy (RBS) and X-ray diffraction analyser (XRD). Superconducting transition temperatures were measured by four probe resistance vs temperature measurements.

RESULTS AND DISCUSSIONS

EPMA and RBS measurements suggest that the composition of the films depends strongly on the substrate temperature, target to substrate distance and position of the substrate beneath the magnetron erosion zone. It has also been observed [16] that sputter cleaning of the target for long a time is essential to obtain homogeneous and highly reproducible films. In our experiments we have sputter cleaned the target for 20 hours before making any film. The films, which were made at a substrate temperature of 400°C in the center of the magnetron erosion zone and at a target to substrate distance of 40 mm had an Y:Ba:Cu ratio of 1:2:3 whereas others had an excess of yttrium. Various films deposited under optimum conditions for the present study are YBC01; thickness 3.0 μm, YBC02; thickness 3.0 μm, YBC03; thickness 1.5 μm deposited on sapphire substrates, YBC04; thickness 2.0 μm, YBC05; thickness 0.5 μm deposited on ZrO_2-3% Y_2O_3 substrates and YBC06; thickness 0.5 μm deposited on MgO (100) substrates. RBS spectrum of YBC03 film is shown in figure 1. It was found that in the as deposited film, at the surface (right flank of the figure 1 (a)) as well as at the interface of the film and the sapphire substrate (left flank of the figure 1 (a)), Y:Ba:Cu ratios were, within the experimental accuracy of the RBS method, correct 1:2:3 stoichiometry. Also, the theoretical simulation of a 1.5 μm thick film with composition $Y_1Ba_2Cu_3O_7$, shown by the solid line, does not show any occurrance of interdiffusion between the film and substrate material. However, for the annealed YBC03 film, the RBS spectrum, shown in figure 1 (b) suggests that although the film surface has an Y:Ba:Cu ratio of 1:2:3, the composition at the interface is quite different. The step like structure observed in the as deposited

films is completly washed out (left flank of the figure 1 (b)) which is an indication of the interdiffusion process of the film and substrate material. Similar interdiffusion between film and substrate material can also be seen on the annealed YBC06 films (figure 1 (c)). The interdiffusion between film and substrate material changes the composition of the film near the interface and has a very strong effect on the superconducting properties of the films. A 1.5 µm thick annealed film, YBC03, does not show zero resistance of superconductivity down to 40K. By increasing the film thickness to 3.0 µm and hence reducing the effect of interface near the surface of the film we obtained superconducting films with zero resistance at 87K on sapphire substrates. A similar interdiffusion effect has been found on the annealed YBC05 and YBC04 films where superconducting transition temperature (zero resistance) increases from 74K to 88K as the thickness of the films increases from 0.5 µm to 2.0 µm. The effect of interdiffusion on the annealed YBC06 films seems to be less severe and we obtained 0.5 µm thick superconducting oxide films with zero resistance at 78K and onset temperature at 82K, a very small transition width.

X-ray diffraction patterns of annealed YBC06,YBC04 and YBC01 films are shown in figure 2 (a), (b) and (c) respectively. These patterns suggest that the YBC06 film, where only (002), (003), (005), (006) and (007) peaks with very large relative intensities are present, has a preferred grain growth of a superconducting phase with the c-axis perpendicular to the film surface. The YBC04 film shows some peaks of very small intensities of the (110), (103), (113), (200), (203), (213) peaks etc. along with relatively very large intensities of (002), (003),

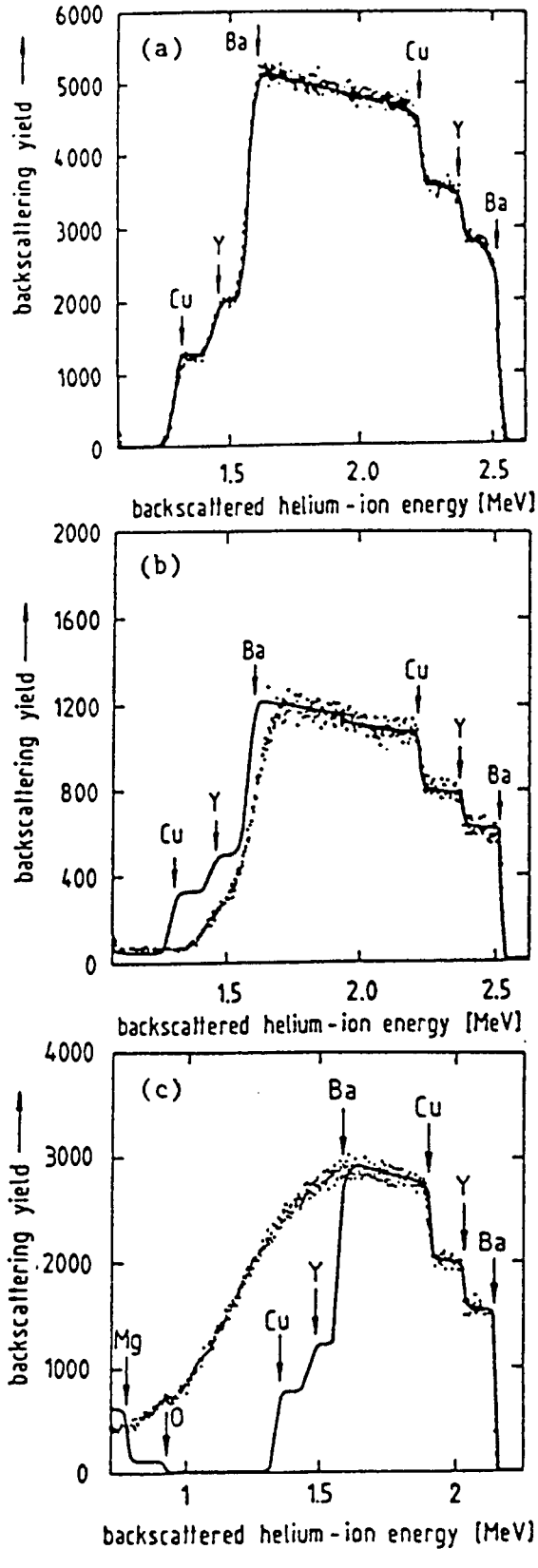

Figure 1 : RBS spectrum of $Y_1Ba_2Cu_3O_7$ films (a) 1.5 µm thick as deposited film on sapphire substrates, (b) 1.5 µm thick annealed film on sapphire substrates and (c) 0.5 µm thick, annealed film on MgO substrates.

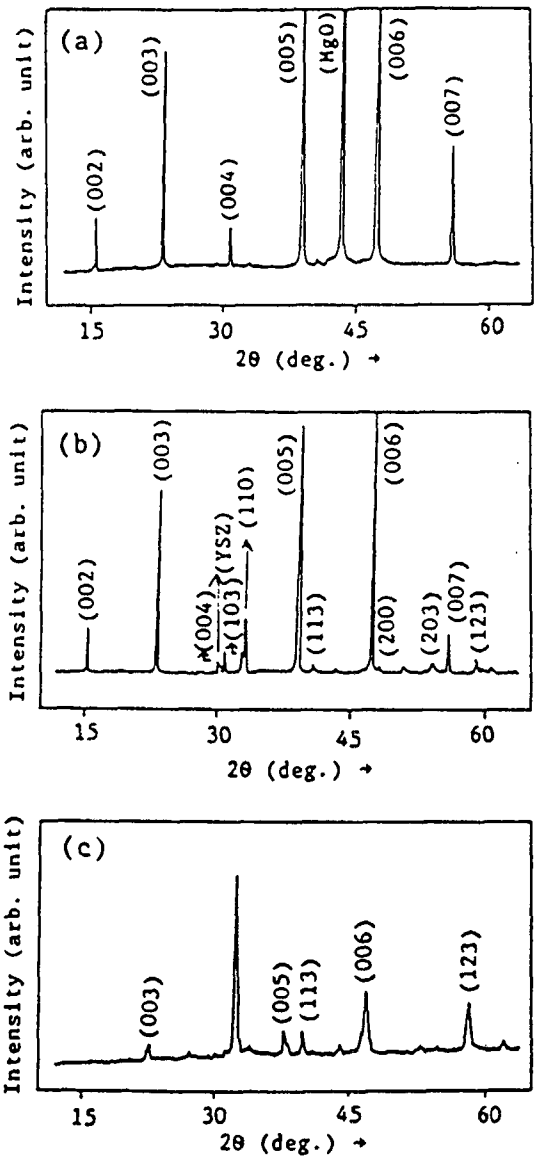

Figure 2 : XRD spectrum of $Y_1Ba_2Cu_3O_7$ films deposited on (a) MgO, (b) ZrO_2-3%Y_2O_3 and (c) sapphire substrates.

(005), (006) and (007) peaks indicating that a small fraction of randomly oriented superconducting phase is present along with a highly c-axis oriented superconducting phase. Splitting of the peaks at 32.5° and 32.8° i.e.(110) and (103) peaks, which is normally observed in bulk superconductors of $Y_1Ba_2Cu_3O_7$ is also present in these films. The relative intensities of (110) and the(103) peaks clearly suggest that major phase present in these films is the orthorhombic phase and not the tetragonal phase.

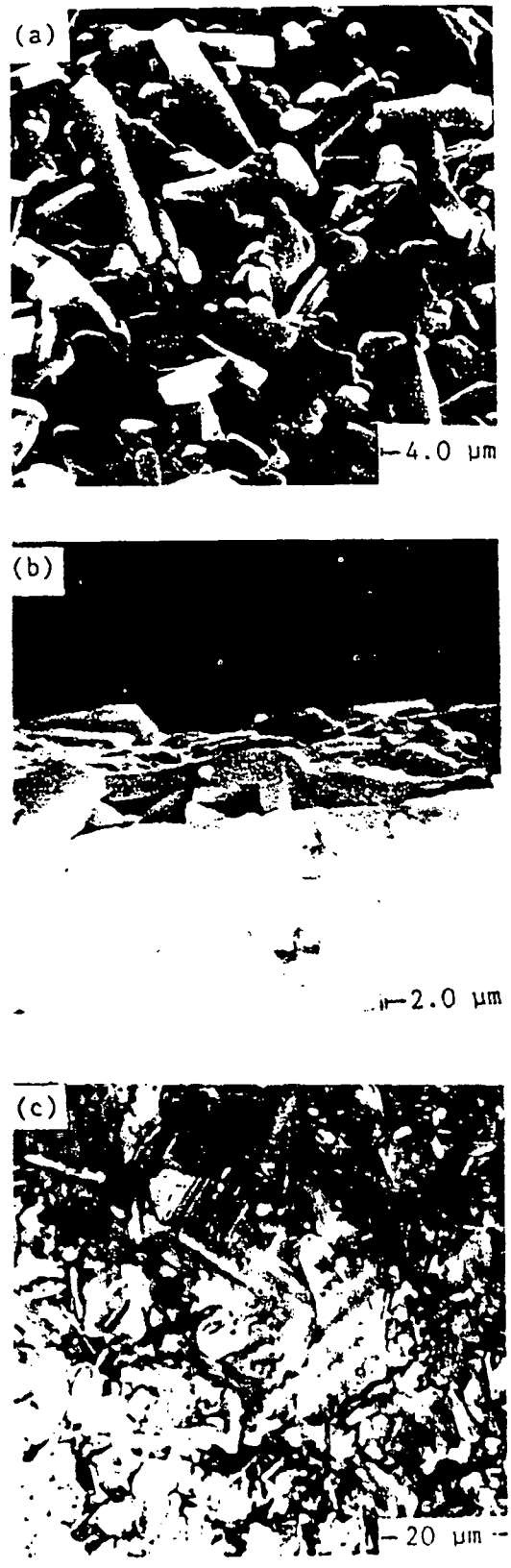

Figure 3 (a) and (b) - SEM pictures of $Y_1Ba_2Cu_3O_7$ film deposited on ZrO_2-3%Y_2O_3 substrates. Figure 3 (c) is the optical micrograph of the same film.

The orthorhombic phase is known to be the superconducting phase responsible for high temperature superconductivity in this class of superconductors. The absence of splitting of the peaks at 32.5° and 32.8° and relatively small intensities of the (003), (005) and (006) peaks observed in X-ray diffraction pattern of the YBC01 film (figure 2 (c)) indicates that this film is randomly oriented and there is no sign of preferred orientation along any axis exist in this film.

Microstructure and fracture cross-section of an annealed YBC04 film as observed by SEM are shown in figure 3 (a) and (b) respectively. It is observed that the as deposited films are microscopically smooth and featureless while the annealed films have various round and rectangular shaped grains overlapping each other. These grains are very large in size ~ 5 - 10 μm. EPMA studies of these grains suggest that they have a correct 1:2:3 ratio of Y:Ba:Cu. An optical micrograph of such a film, taken with polarized light is shown in figure 3 (c). It reveals that the grains in these films have various twinnings. A systematic study of these twins, done by other groups [17, 19] suggest that the twins are formed at the tetragonal to orthorhombic transition temperature ~600°C. We have not observed these twins on the films deposited on sapphire and MgO substrates.

The superconducting transitions, as seen in d.c. resistance vs temperature measurements, of the various films YBC01 to YBC06 are shown in figure 4. It is observed that the YBC01, YBC04, YBC05 and YBC06 films are metallic in the normal state. Their resistivity at 100K is 4.5 mΩ·cm, 1·3 mΩ cm, 0.7 mΩ cm and 220 μΩ cm respectively. YBC01, YBC04 and YBC06 films show very small transition widths of 6K, 7K and 4K respectively, whereas YBC05 film shows a relatively large transition width of 17K. Also the superconductivity set in T_c (on set) at 93 K and 95 K for YBC01 and YBC04 films, they become fully superconducting (Tc(zero)) at 87K and 88K respectively, whereas Tc (onset) and Tc(zero) are at 92K and 74K for YBC05 films and at 82K and 78 K for YBC06 films. The resistance vs temperature measurements for the YBC02 and YBC03 films are quite different where we observed a semi-conducting behaviour in the normal state of these films. For the YBC02 film, Tc (onset) is at 95K. The resistance of this film reaches half of its normal state value at 92 (Tc (midpoint)) which is even 2K higher than for the YBC01 film, but it shows a long resistive tail extending down to 76K. The Tc (zero) for the YBC03 film however sets in at a much lower temperature, below 40K.

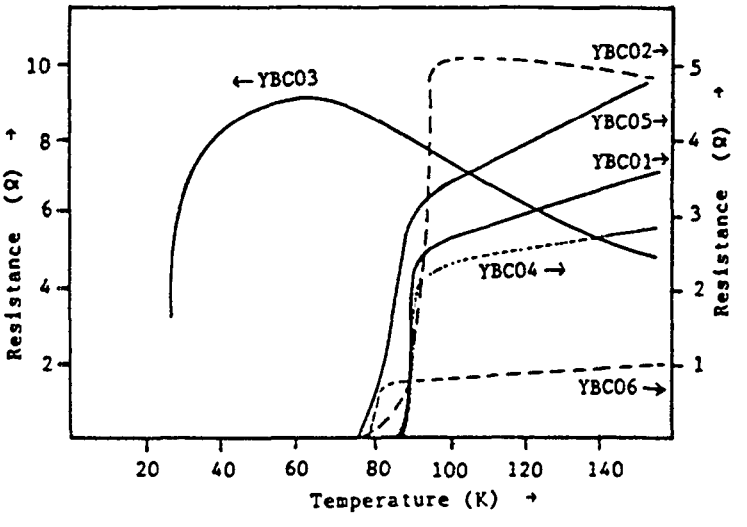

Figure 4 : d.c. resistance vs temperature dependance of various $Y_1Ba_2Cu_3O_7$ films.

CONCLUSIONS

R.f. magnetron sputtering from a single stoichiometric target has been used to obtain superconducting oxide films of $Y_1Ba_2Cu_3O_7$. By optimizing

various sputtering parameters and annealing conditions films with T_c (onset) at 95K, 93K and 82K with Tc(zero) at 88 K, 87 K and 78K have been obtained on ZrO_2-3%Y_2O_3, sapphire and MgO substrates, respectively. The films deposited on MgO substrates show a preferred grain growth of a superconducting phase with c-axis perpendicular to the film surface whereas films deposited on ZrO_2-3%Y_2O_3 substrates show a small fraction of randomly oriented superconducting phase along with c-axis oriented superconducting phase. The films deposited on sapphire substrates are randomly oriented.

REFERENCES

1. J.G. Bednorz and K.A. Müller, Z. Phys. B 64, 189 (1986)
2. C.W. Chu, P.H.Hor, R.L. Meng, L. Gao, Z.J. Huang and Y.Q. Wang, Phys. Rev. Lett. 58, 405 (1987)
3. P.Chaudhari, R.H. Koch, R.B. Laibowitz, T.R. McGuire and R.J. Gambino, Phys. Rev. Lett. 58, 2684 (1987)
4. Y. Enomoto, T. Murakami, M. Suzuki and K. Moriwaki, Jpn. J. Appl. Phys. 26, L1248 (1987)
5. S.J. Lee, E.D. Rippert, B.Y. Jin, S.N. Song, S.J. Hwu, K. Poeppelmeier and J.B. Ketterson, Appl. Phys. Lett. 51, 1194 (1987)
6. H. Adachi, K. Setsune, T. Mitsuyu, K. Hirochi, Y. Ichikawa, T. Kamada and K. Wasa, Jpn. J. Appl. Phys. 26, L709 (1987)
7. S.H. Liou, M. Hong, J. Kwo, B.A. Davidson, H.S. Chen, S. Nakahara, T. Boone and R.J. Felder, Appl. Phys. Lett. 52, 1735 (1988)
8. T. Akune and N. Sakamoto, Jpn. J. Appl. Phys. 27, L2078 (1988)
9. T. Aida, T. Fukazawa, K. Takagi and K. Miyauch, Jpn. J. Appl. Phys. 26, L1489 (1987)
10. H. Asano, T. Tanabe, Y. Katoh, S. Kubo and O. Michikami, Jpn. J. Appl. Phys. 26, L1221 (1987)
11. M. Gurvich and A.T. Fiory, Appl. Phys. Lett. 51, 1027 (1987)
12. K. Char, A.D. Kent, A. Kapitulnik, M.R. Beasley and T.H. Geballe, Appl. Phys. Lett. 51, 1370 (1987)
13. R.M. Silver, J. Talvacchio and A.L. de Lozanne, Appl. Phys. lett. 51, 2149 (1987)
14. P.K. Srivastava, P. Debély, H.E. Hintermann, C. Leemann, J. Weber, O. Caccivio, P. Martinoli, H.R. Ott, Physica C 153-155, 1443 (1988)
15. P.K. Srivastava, P. Debély, H.E. Hintermann, C. Leemann, Ph. Flückiger, O. Caccivio, J.-L. Gavilano, J. Weber and P. Martinoli, Paper presented at Int. Conf. on Appl. Superconductivity held at San Francisco, CA. U.S.A. on 21-25 Aug. (1988)
16. T.I. Selinder, G. Larsson, U. Helmerson, P. Olsson, J.E. Sundgren and S. Rudner, Appl. Phys. Lett. 52, 1907 (1988)
17. K. Tachikawa, N. Sadakata, M. Sugimoto and O, Kohno, Jpn. J. Appl. Phys. 27, L1501 (1988)
18. J.J. Chu, R.S. Liu, J.H. Kung, P.T. Wu and L.J. Chen, J. Appl. Phys. 64, 2523 (1988)
19. T. Sawada, H. Takei, S. Takekawa, K. Kitamura, S. Kimura and N. Iyi, Jpn. J. Appl. Phys. 27, L 1184 (1988)

NORTH-HOLLAND
PHYSICS
PUBLISHING

PENETRATION DEPTH IN YBaCuO FILMS

Ph. FLUECKIGER[1], J.-L. GAVILANO[1], Ch. LEEMANN[1], P. MARTINOLI[1], B. DAM[2], G.M. STOLLMAN[2], P.K. SRIVASTAVA[3], P. DEBELY[3], and H.E. HINTERMANN[3]

[1] Institut de Physique, Université de Neuchâtel, CH-2000 Neuchâtel, [2] Philips Research Laboratories, P.O. Box 80.000, NL-5600 JA Eindhoven, and [3] CSEM, CH-2000 Neuchâtel

With a two coil mutual inductance technique the in plane penetration depth in compact YBaCuO films was measured to be $\lambda(0) \approx 0.23$ μm. In granular YBaCuO films the penetration depth is larger, its value being determined by the strength of the intergranular Josephson coupling energy.

Reprinted from PHYSICA C

Physica C 162-164 (1989) 1563-1564
North-Holland

PENETRATION DEPTH IN YBaCuO FILMS

Ph. FLUECKIGER[1], J.-L. GAVILANO[1], Ch. LEEMANN[1], P. MARTINOLI[1], B. DAM[2], G.M. STOLLMAN[2], P.K. SRIVASTAVA[3], P. DEBELY[3], and H.E. HINTERMANN[3]

[1] Institut de Physique, Université de Neuchâtel, CH-2000 Neuchâtel, [2] Philips Research Laboratories, P.O. Box 80.000, NL-5600 JA Eindhoven, and [3] CSEM, CH-2000 Neuchâtel

With a two coil mutual inductance technique the in plane penetration depth in compact YBaCuO films was measured to be $\lambda(0) \approx 0.23$ μm. In granular YBaCuO films the penetration depth is larger, its value being determined by the strength of the intergranular Josephson coupling energy.

It has been suggested[1] that the high temperature superconducting ceramic $YBa_2Cu_3O_7$, owing to its large a-b vs c anisotropy, can be modelled as a system of weakly coupled two dimensional (2D) Josephson junction arrays located in the CuO_2 planes. Such intrinsic array-like behavior may however often be masked by an extrinsic one : Josephson weak link effects at the grain boundaries. The fundamental physical parameter, whose temperature dependence will reflect renormalization effects caused by 2D phase fluctuations, is the penetration depth λ. In the present letter we compare the temperature and magnetic field dependence of λ, measured with a two coil mutual inductance technique[2], in a compact and in an extremely granular YBaCuO film.

The compact sample S1, 0.1 μm thick, was deposited in a UHV triple e-beam system onto a (100) $SrTiO_3$ substrate, the granular sample S2, 0.5 μm thick, was deposited with single target magnetron sputtering onto a MgO substrate. The details of both processing methods have been published elsewhere[3,4]. Both films were subjected to x-ray analysis showing that they were c-axis oriented (i.e. the c-axis was perpendicular to the film surface). Rutherford backscattering (RBS) analysis showed that while S1 had the correct 1:2:3 stoichiometry, accurate to within 10%, sample S2 had a small excess of Cu indicating, possibly, an admixture of the 2:4:8 phase. In the normal state both samples had a metallic resistance vs temperature dependence and the resistivity at T_c^+ was 50 μΩcm and 350 μΩcm for S1 and S2 respectively.

The penetration depth λ of the films was deduced from a measurement of their screening properties with an inductive method [2,5]. The sample is positioned directly under a coil assembly consisting of an excitation coil and a concentric gradiometer detection coil. Screening currents, induced with the excitation coil, induce a signal in the detection coil which can be phase-sensitively detected. In our measurements, the frequency of the drive current was 3 kHz and its amplitude small enough to assure linear response. With a relatively simple numerical procedure it is then possible to extract the sample's complex conductance G from the in-phase , $Re(\delta V)$, and the quadrature , $Im(\delta V)$, components of the measured signal voltage. For the sample's conductance we write $G^{-1} \equiv Z(\omega) = R+i\omega L_K$; the "resistance" R comprising all possible sources of dissipation : normal currents, flux flow, phase fluctuations, etc. The sheet kinetic inductance L_K is the quantity of interest here, since it is directly related to the penetration depth λ by $L_K = \mu_0\lambda^2/d$ with d the thickness of the film[5]. Figure 1 shows the temperature dependence of λ for the two samples S1 and S2 and (solid and dashed lines) the fits to expression $\lambda(T) = \lambda(0) \cdot (1-T/T_0)^{-1/2}$. Fitting parameters are $\lambda(0) = 0.23$ μm, $T_0 = 89$ K for sample S1 and $\lambda(0) = 0.54$ μm, $T_0 = 78$ K for sample S2. The lower

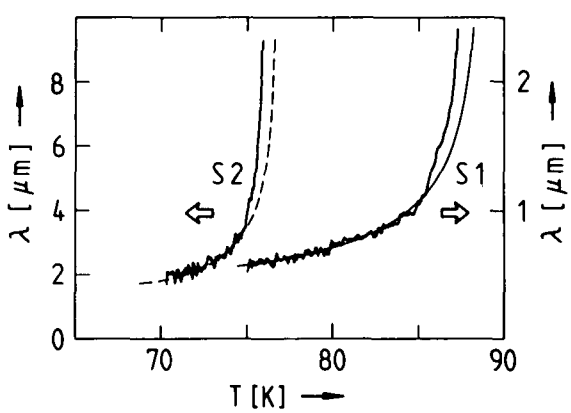

FIGURE 1
Temperature dependence of the penetration depth λ for a compact (S1) and a granular (S2) YBaCuO film. Solid and dashed lines are fits to the expression $\lambda(T) = \lambda(0)\cdot(1-t)^{-1/2}$

mean field transition temperature T_0 of sample S2 could be an indication of its granular nature (see below) or, more likely, due to an admixture of the 2:4:8 phase, as already indicated by the RBS data. Close to T_0 the measured λ deviate from the fit, a behavior which can be, at least qualitatively understood in terms of a renormalisation of the superfluid density by phase fluctuations[6]. Aside from this expected high temperature deviation, the fit of the data to the mentioned expression is, for sample S1, remarkably good in the investigated temperature range. The value $\lambda(0) = 0.23$ μm may thus be identified with the zero temperature value of the in plane penetration depth λ_{ab}, to be compared with other measurements of this parameter [6,7]. Sample S2, on the other hand, shows a deviation from the fit not only close to T_0, but also at low temperatures, the measured λ being consistently larger than the fit. We believe that in this case a more complicated theoretical expression for λ should be envisioned, taking into account the granular nature of this film. Presumably, the effective λ_{eff} would in this case consist of λ_{ab}, as for S1, and of an intergrain penetration depth λ_g.

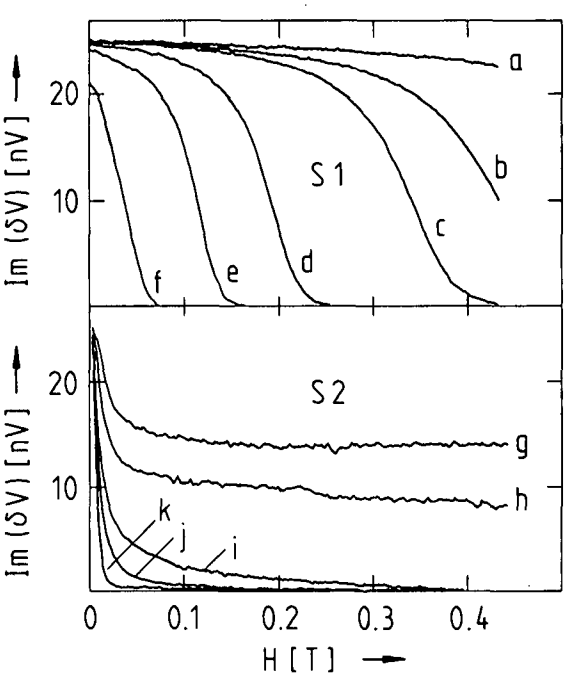

FIGURE 2
Imaginary part of the signal voltage as a function of transverse magnetic field for samples S1 and S2. The reduced temperatures labeled a to f are 0.95, 0.96, 0.965, 0.97, 0.975,0.98; g to k are 0.50, 0.65, 0.78, 0.82, and 0.86

Since the kinetic inductance is the additive quantity, one might expect the following relationship between the various λ : $\lambda^2_{eff} = \lambda^2_{ab} + \lambda^2_g$. A more detailed analysis of the penetration depth in granular films will be presented elswehere.

The most dramatic difference in behavior of the two samples was observed in a perpendicular magnetic field. Figure 2 shows the imaginary part of the signal voltage as a function of magnetic field at different reduced temperatures $t \equiv T/T_0$. Notice that the magnetic field can penetrate into sample S1 only at the highest temperatures : intrinsic YBaCuO properties are measured in this compact sample. Owing to the large upper critical field, up to $t \sim 0.95$ a magnetic field of 0.5 T has practically no effect on its screening properties.

By contrast the data for S2 exhibit a sharp drop at low magnetic fields at all temperatures shown, down to $t = 0.5$. This initial drop, occurring at a very weakly temperature dependent magnetic field of 200-300 G, can be attributed to a decoupling of the individual grains at low magnetic fields. If we identify this field as the field necessary to nucleate one flux quantum in the junctions between the grains, with the given sample thickness the junction width turns out to be a few tenths of a μm, slightly less than the grain size estimated from optical and scanning electron micrographs.

In conclusion, inductive conductance measurements in compact YBaCuO films have yielded an in plane penetration depth $\lambda(0) = 0.23$ μm. As a function of temperature, λ closely follows a $(1-t)^{-1/2}$ law. In granular films the temperature dependence of λ is more complex, the present analysis yielding only a lower limit for $\lambda(0)$.

This work was supported by the Swiss National Science Foundation.

REFERENCES

1. G. Deutscher and K. A. Müller, Phys. Rev. Lett 59 (1987) 1745
2. A.T. Fiory et al., Appl. Phys. Lett. 52 (1988) 2165
3. B. Dam et al., Proc. Am. Vacuum Soc., Atlanta, October 1988
4. P.K. Srivastava et al., IPAT 89 Conference Proceedings (Page Bros, Norwich 1989) p. 361
5. P. Martinoli et al., Jpn. J. Appl. Phys. 26, Suppl. 26-3 (1987) 1999
6. A.T. Fiory, et al., Phys. Rev. Lett. 61 (1988) 1419
7. D.R. Harshman et al., Phys. Rev. B 36 (1987) 2386

Percolative Behavior of the Superconductive Transition of $YBa_2Cu_3O_7$ Films

Ch. Leemann, Ph. Flückiger, V. Marsico, J. L. Gavilano,[a] P. K. Srivastava, Ph. Lerch, and P. Martinoli
Institut de Physique, Université de Neuchâtel, 2000 Neuchâtel, Switzerland
(Received 30 March 1990)

The superconductive transition of c-axis-oriented $YBa_2Cu_3O_7$ thin films, as characterized by measurements of the temperature dependence of the magnetic penetration depth, is found to occur below the Ginzburg-Landau mean-field transition. The divergence of the penetration depth at the transition is in good quantitative agreement with the predictions of a percolation model.

PACS numbers: 74.50.+r, 74.70.Mq

Scanning electron micrographs of high-temperature superconducting ceramics create the impression of a conglomerate of grains of size ~ 1 μm, thereby requiring the necessity to incorporate granularity in the description of these materials and their physical properties. Coupled with the knowledge of a pathologically short coherence length, of the order of 10 Å,[1] which in no way can smooth out the grainy structure, this leads quite naturally to modeling these ceramics as networks of grains coupled by Josephson weak links.[2,3] Of course such a picture does not preclude the existence of intrinsic weak-link effects within the material itself, as postulated by Deutscher and Müller,[4] which are, however, if at all, only observable with the utmost care and precaution in single-crystal samples. Under normal circumstances the strength (or weakness) of the grain-to-grain coupling is expected to play a dominant role in determining macroscopic transport properties. In this paper we present measurements of the penetration depth in two-dimensional (2D), c-axis-oriented $YBa_2Cu_3O_7$ (YBCO) films. These measurements are in excellent agreement with a percolation description of the films, based on the assumptions that the grains are coupled via the usual Ambegaokar-Baratoff[5] tunnel-junction formula and that the normal-state junction resistances R_n obey a Gaussian distribution. The characteristic features of 2D critical fluctuations in the form of a Kosterlitz-Thouless-Berezinski (KTB) vortex unbinding transition,[6] in principle present and observed in some cases,[7-10] are completely masked by the much more prominent consequences of random coupling between the grains.

Thin films of YBCO were deposited onto polished $SrTiO_3$ (100) substrates with an *in situ* (no annealing) process using cylindrical "hollow cathode" magnetron single-target sputtering.[11] After some fine tuning, this method was found to produce superior quality films. The transport critical current density in these films increases sharply below the mean-field transition temperature T_{c0}, to reach 10^6 A/cm^2 at, typically, a reduced temperature $T/T_{c0} \simeq 0.8$. In the following we will consider one representative film of thickness $d \sim 200$ Å as determined by Rutherford backscattering spectrometry. X-ray analysis showed that the film was c-axis oriented. The effective thin-film penetration depth $\Lambda = 2\lambda^2/d$, where λ is the bulk in-plane penetration depth, was deduced from measurements of the film's screening properties.[12,13] The film is positioned directly underneath a cylindrical excitation coil and a coaxial gradiometer detection coil. A current flowing in the excitation coil induces screening currents in the film which in turn induce a signal in the detection coil. From this signal, measured phase sensitively, the complex sample impedance $Z = R + i\omega L_k$ can be extracted[13] and thus Λ from the sheet kinetic inductance L_k, since $\Lambda = 2L_k/\mu_0$. In Fig. 1 the in-phase, $\mathrm{Re}\delta V$, and quadrature, $\mathrm{Im}\delta V$, components of the signal voltage measured at a frequency of 3 kHz are shown as a function of temperature, and, on a different temperature scale but with a common point at 79 K, the result of a four-probe van der Pauw measurement of the dc resistive transition. For these measurements, the ambient magnetic field was reduced to ~ 1 mG with Mu-metal shielding. The relatively low T_{c0} (79 K) is probably caused by the thinness of the film; thicker films ($d \geq 1000$ Å) prepared with the same processing method had, typically, a T_{c0} of 90 K. The choice of such a thin film was dictated by the need to increase Λ in order to improve the

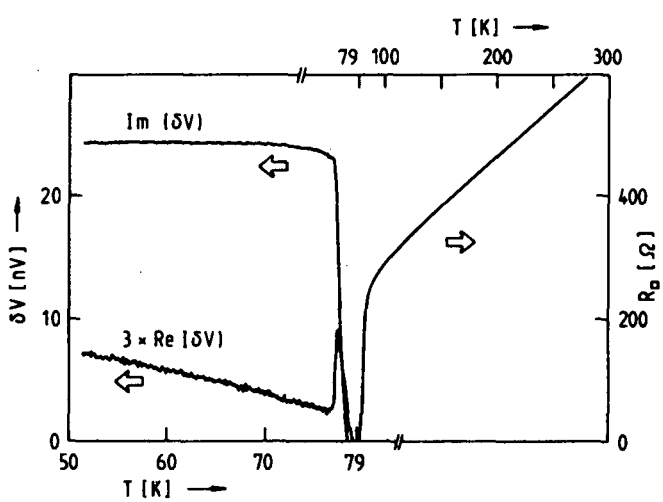

FIG. 1. Real, $\mathrm{Re}\delta V$, and imaginary, $\mathrm{Im}\delta V$, parts of the signal voltage measured at 3 kHz and the sheet resistance as a function of temperature. Note the different temperature scales for the resistive and inductive data, with a common point at $T = 79$ K.

measurement sensitivity. Notice that the inductive response starts with the sheet resistance $R_\square \simeq 0$, and that the $\mathrm{Re}\delta V(T)$ component, characterized by a peak at the transition, exhibits a low-temperature tail not normally observed in such measurements.[13] In Fig. 2 the result of the analysis outlined above, applied to the measurement of Fig. 1, is shown together with the dc resistive transition on the same temperature scale. The temperature dependence of Λ^{-1} is linear below ~ 75 K and there is a "jump" to zero setting in at ~ 76 K. Except very close to T_{c0}, the screening properties of the film were found to be quite insensitive to weak (up to 0.5 T) magnetic fields. Together with the sharpness of both the resistive and inductive transitions, this demonstrates the good quality of this very thin film.

While the film's properties presented above demonstrate that it certainly is not a system of loosely coupled grains, we nonetheless assume that, at least in the transition region, granularity is the key feature. Accordingly, for the interpretation of the temperature dependence of Λ^{-1} presented in Fig. 2, we follow the basic ideas set forth by Deutscher *et al.*[14] and Ebner and Stroud.[15] All the individual grains in the film become superconducting at the same temperature T_{c0}; however, two grains are coupled only when the Josephson coupling energy E_J exceeds the thermal energy kT. Charging effects are neglected: The high transition temperature, the relatively large grain size and the not exceedingly large junction resistance guarantee that, at least in the transition region, the charging energy $E_c \ll kT$. Then, if the coupling between the grains follows some statistical distribution function, the superconducting transiton becomes a bond percolation problem. As the temperature is lowered, the fraction p of coupled grains increases, the exact functional relationship $p(T)$ being determined by the choice of the independent random variable and its distribution function. Since in our experiments we measure $\Lambda(T)$, in order to interpret the measurements in terms of a percolation model, an expression for $\Lambda(p(T))$ is necessary. In Ref. 15 the helicity modulus Γ (proportional to the superfluid density and hence to Λ^{-1}) in a three-dimensional (3D) site-diluted granular superconductor was shown to be proportional to the normal-state conductivity σ:

$$\Gamma(p)/\Gamma(1) = \sigma(p)/\sigma(1) . \tag{1}$$

The grain size being of the order of 1 μm and the film thickness ~ 200 Å, the percolation dimensionality is 2. The validity of Eq. (1) was demonstrated by showing that, at a given percolation probability, the superfluid density is proportional to the conductance of the sample in the normal state.[15] It appears reasonable to assume that this result, and therefore Eq. (1), is true in 2D as well as 3D. A further *caveat* concerning Eq. (1) should be mentioned: It is valid only at low temperatures, below the critical region where fluctuations in the phase of the superconducting order parameter renormalize Γ. As we will see, the percolative transition occurs below this critical temperature regime in our samples. The use of Eq. (1) appears thus to be justified and we expect Λ to diverge with the conductivity exponent t:[16]

$$\Lambda(p) = \Lambda(1)\frac{1}{|p-p_c|^t} , \tag{2}$$

where p_c is the percolation threshold.

For the derivation of $p(T)$, we assume that the normal-state grain-grain resistances R_n obey a Gaussian centered at R_{av}, with standard deviation δR. The junction coupling energy is given by[5]

$$E_J = \frac{h}{8e^2 R_n}\Delta(T)\tanh\frac{\Delta(T)}{2kT} , \tag{3}$$

an expression applicable not only to tunnel junctions, but also, e.g., to metallic weak links.[17] Since everything of interest happens close to T_{c0}, we expand the gap parameter $\Delta(T)$ and the tanh function to find

$$E_J = \frac{R_0}{R_n}k\delta T \tag{4}$$

valid for $\delta T \equiv T_{c0} - T \ll T_{c0}$, with $R_0 = 3.7\hbar/e^2$. The condition for superconducting coupling between two grains $E_J \geq kT$ now reduces to $R_n \leq R_0\delta T/T$. The fraction of grain-grain resistances less than R_n being given by $\mathrm{erf}[(R_n - R_{\mathrm{av}})/\delta R)]$, where

$$\mathrm{erf}(x) \equiv \frac{1}{\sqrt{2\pi}}\int_{-\infty}^{x} e^{-y^2/2}dy ,$$

we arrive at the result

$$p(T) = \mathrm{erf}\left[\frac{R_0\delta T/T - R_{\mathrm{av}}}{\delta R}\right] . \tag{5}$$

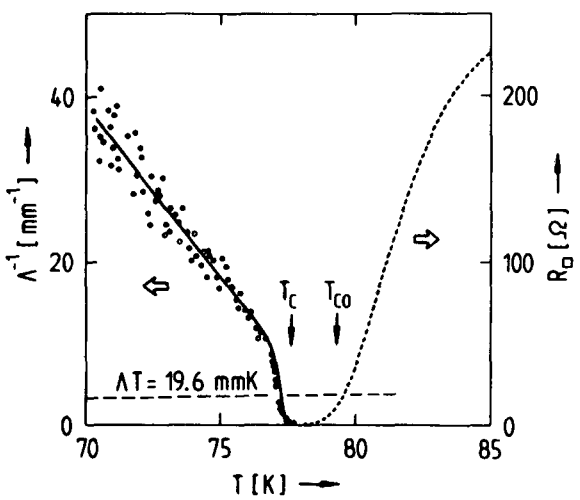

FIG. 2. Temperature dependence (circles) of Λ^{-1} deduced from the measurement of Fig. 1 and (solid line) the fit for Λ^{-1} according to Eq. (7). The dotted line above T_c is the resistive transition. T_{c0} is given by the extrapolation to zero of the linear part of Λ^{-1}; T_c was determined from the fit and Eq. (6). The dashed line is the Kosterlitz-Thouless prediction $\Lambda(T_c)T_c = 19.6$ mm K.

Zero resistance is reached when $p(T)=p_c$, a condition which, for $p_c=0.5$, results in a temperature T_c given by

$$T_c = T_{c0}\frac{R_0}{R_0+R_{av}} \simeq T_{c0}\left(1-\frac{R_{av}}{R_0}\right), \quad (6)$$

since $R_{av} \ll R_0$. With a slightly different R_0 value, this is the same relationship for the reduction of T_c as in a superconducting film undergoing a KTB transition.[18] The final result for the temperature dependence of Λ is thus

$$\Lambda(T) = \frac{\Lambda(0)}{2(1-T/T_{c0})}\frac{p_0}{|p(T)-p_c|^t}, \quad (7)$$

where $p_0=|p(0)-p_c|^t$ ensures the consistency of the equation at $T=0$, and $p(T)$ is given by Eq. (5). Since in YBCO the mean free path is larger than the coherence length, we have used the clean limit expression for $\Lambda(T)$ in the Ginzburg-Landau regime,[19] leading to the factor of 2 in the denominator of Eq. (7).

The solid line in Fig. 2 is a numerical calculation of $\Lambda^{-1}(T)$ with Eqs. (5), (7), and the explicit expression for erf(x) given above. The fitting parameters $\Lambda(0)=6.0$ μm and $T_{c0}=79.3$ K are determined by the straight, low-temperature section of the curve. The two arrows in Fig. 2 indicate the temperatures T_{c0} and $T_c=77.4$ K, as determined with Eq. (6). The $\Lambda(0)$ value corresponds to $\lambda(0)=0.24$ μm, a zero-temperature penetration depth comparable to the monocrystalline in-plane $\lambda=0.14$ μm.[20] Since the fit is quite insensitive to changes of the parameters p_c and t, these two were kept fixed at the 2D bond percolation values $p_c=0.5$ and $t=1.3$ (Ref. 16) for all samples investigated. Thus, for the fit of $\Lambda^{-1}(T)$ in the critical region there are effectively only two adjustable parameters: R_{av} and δR, which were found to be 345 and 60 Ω, respectively. Notice that the theoretical curve correctly describes the divergence of Λ up to $\Lambda \sim 1$ mm. Large-scale sample inhomogeneities and fluctuation effects are probably responsible for the observed rounding of the foot of the $\Lambda^{-1}(T)$ curve. The value found for R_{av} is slightly too large when compared with the measured dc sheet resistance of $R_\square=250$ Ω. In other samples the difference was even more pronounced, but always $R_{av}>R_\square$. This systematic discrepancy is possibly due to a reduction of the coupling energy caused by a lowering of the gap parameter Δ at the grain surfaces,[4] which is equivalent to a smaller R_0 in Eq. (4), and hence to a smaller R_{av} in our analysis. Also shown in Fig. 2 is a dashed line corresponding to the universal KTB prediction $\Lambda(T_c)T_c=19.6$ mm K for the value of Λ at the jump. In all samples investigated so far, the jump at T_c was at least a factor of 2 larger than expected for a KTB transition, thereby showing that the percolative transition occurs below the temperature regime dominated by fluctuation effects and providing an *a posteriori* justification for the use of Eq. (1). Moreover, calculations based on the KTB recursion relations at nonzero frequencies[17,21] always predict much sharper transitions than the observed ones.

Additional evidence for the percolation interpretation of the superconducting transition of YBCO films is, at least qualitatively, provided by an analysis of the dissipation present in the films below T_c. In almost all the samples investigated so far we have observed below the transition a monotonic increase of ReδV with decreasing temperature, as shown by the Re$\delta V(T)$ curve of Fig. 1. In part, this effect is a measurement artifact: the temperature dependence of the resistances of the measuring coils, which causes a temperature-dependent variation of the phase angle in the detection system.[13] Taking this effect into account in the analysis results in a small and negligible error in the determination of $\Lambda^{-1}(T)$, but results in an appreciable error in the Re$Z(T)$ curve. The absolute level of the Re$Z(T)$ curve shown in Fig. 3 is thus somewhat uncertain; however, with a noise floor of ~ 0.1 $\mu\Omega$, it clearly shows that there is a large temperature regime *below* the transition with nonvanishing dissipation. This is in qualitative agreement with the result of a Monte Carlo calculation of the frequency-integrated real part of the fluctuation conductivity of model granular superconductor,[15] where disspation below T_c was found to arise from the presence of disorder, possibly in the form of dangling bonds. The dissipation observed in our YBCO films below the transition region would then be the consequence of the percolation probability[16] being less than unity, but slowly increasing with decreasing temperature, to finally reach unity at ~ 50 K. This in turn implies that there are more (a few percent) high-resistance junctions than predicted by a Gaussian distribution with the mean and the standard deviation found above.

In a percolation description of the superconductive transition one would expect the initial rise of resis-

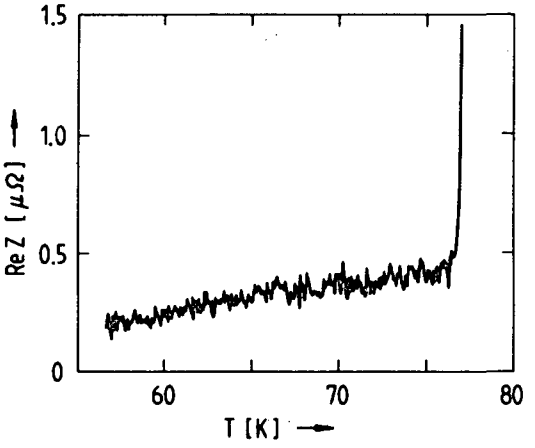

FIG. 3. ReZ as a function of temperature deduced from the measurement of Fig. 1, showing non-negligible dissipation down to ~ 50 K.

tance to be, at least approximately, given by $R_{\square}(T) \simeq R_{\mathrm{av}}|p(T)-p_c|^t$. The resistive transitions of our YBCO films do not fit such an expression. This is probably due to a distribution of the single-grain transition temperatures T_{c0} and, more importantly, to the increasing importance of thermal fluctuations leading to effects such as phase slippage across grain boundaries[22] and order-parameter amplitude fluctuations.[23] These effects dominate the resistive transition rendering the effect of percolative coupling between the grains secondary and observable only *below* T_c, where almost all the grains are superconducting and amplitude fluctuations frozen out. This is consistent with the observation that a percolation description of the resistive transition is successful in cases where the transition is split into two sections, with a tail extending into a temperature regime without order-parameter amplitude fluctuations.[24]

In conclusion, both the attractive simplicity of the model presented in this paper and the excellent agreement between the predictions of the model and the measured temperature dependence of the penetration depth provide strong support for the description of the superconductive transition of YBCO films with a percolation model. We dismiss an interpretation of our data in terms of a vortex unbinding transition, since the observed jump in superfluid density at the transition is always too large and the transition region wider than expected. Unfortunately we are not able to verify that, as predicted by Ebner and Stroud,[15] the exponent describing the divergence of Λ at the percolation threshold is indeed the conductivity exponent.

J. Weber's Rutherford backscattering spectroscopy measurements and analyses are gratefully acknowledged, as well as P. Debély's valuable technical assistance in the early stages of this project. This work was supported by the Swiss National Science Foundation.

---

[a]Present address: Laboratorium für Festkörperphysik, Eidgenössische Technische Hochschule Zürich-Hönggerberg, 8093 Zürich, Switzerland.

[1]T. K. Worthington, W. J. Gallagher, and T. R. Dinger, Phys. Rev. Lett. **59**, 1160 (1987).

[2]J. R. Clem, Physica (Amsterdam) **153–155C**, 50 (1988).

[3]R. L. Peterson and J. W. Ekin, Phys. Rev. B **37**, 9848 (1988).

[4]G. Deutscher and K. A. Müller, Phys. Rev. Lett. **59**, 1745 (1987).

[5]V. Ambegaokar and A. Baratoff, Phys. Rev. Lett. **10**, 486 (1963).

[6]J. M. Kosterlitz and D. J. Thouless, J. Phys. C **6**, 1181 (1973).

[7]A. T. Fiory, A. F. Hebard, P. M. Mankiewich, and R. E. Howard, Phys. Rev. Lett. **61**, 1419 (1988).

[8]S. Martin, A. T. Fiory, R. M. Fleming, G. P. Espinosa, and A. S. Cooper, Phys. Rev. Lett. **62**, 677 (1989).

[9]D. H. Kim, A. M. Goldman, J. H. Kang, and R. T. Kampwirth, Phys. Rev. B **40**, 8834 (1989).

[10]N.-C. Yeh and C. C. Tsuei, Phys. Rev. B **39**, 9708 (1989).

[11]X. X. Xi, G. Linker, O. Meyer, and J. Geerk, J. Less-Common Met. **151**, 349 (1989).

[12]A. T. Fiory, A. F. Hebard, P. M. Mankiewich, and R. E. Howard, Appl. Phys. Lett. **52**, 2165 (1988).

[13]B. Jeanneret, J. L. Gavilano, G.-A. Racine, Ch. Leemann, and P. Martinoli, Appl. Phys. Lett. **55**, 2336 (1989).

[14]G. Deutscher, O. Entin-Wohlman, S. Fishman, and Y. Shapira, Phys. Rev. B **21**, 5041 (1980).

[15]C. Ebner and D. Stroud, Phys. Rev. B **28**, 5053 (1983).

[16]S. Kirkpatrick, Rev. Mod. Phys. **45**, 574 (1973).

[17]B. Jeanneret, Ph. Flückiger, J. L. Gavilano, Ch. Leemann, and P. Martinoli, Phys. Rev. B **40**, 11 374 (1989).

[18]M. R. Beasley, J. E. Mooij, and T. P. Orlando, Phys. Rev. Lett. **42**, 1165 (1979).

[19]M. Tinkham, *Introduction to Superconductivity* (McGraw-Hill, New York, 1975).

[20]D. R. Harshman, L. F. Schneemeyer, J. V. Waszczak, G. Aeppli, R. J. Cava, B. Batlogg, L. W. Rupp, E. J. Ansaldo, and D. Ll. Williams, Phys. Rev. B **39**, 851 (1989).

[21]V. Ambegaokar, B. I. Halperin, D. R. Nelson, and E. D. Siggia, Phys. Rev. B **21**, 1806 (1980).

[22]R. Gross, P. Chaudhari, D. Dimos, A. Gupta, and G. Koren, Phys. Rev. Lett. **64**, 228 (1990).

[23]D. H. Kim, A. M. Goldman, J. H. Kang, K. E. Gray, and R. T. Kampwirth, Phys. Rev. B **39**, 12275 (1989).

[24]C. J. Lobb, M. Tinkham, and W. J. Skocpol, Solid State Commun. **27**, 1273 (1978).

Physica B 165&166 (1990) 1163–1164
North-Holland

Vortex Dynamics in $YBa_2Cu_3O_7$ Films

P. Martinoli, Ph. Flückiger, V. Marsico, P.K. Srivastava, Ch. Leemann, and J. L. Gavilano*,

Institut de Physique, Université de Neuchâtel, 2000 Neuchâtel, Switzerland

The low frequency complex ac impedance Z of c-axis oriented $YBa_2Cu_3O_7$ thin films was measured as a function of the applied magnetic field B. At temperatures not too close to the transition temperature the imaginary part of Z is proportional to B^2, while the real part consists of a term proportional to B^3 and an additional term proportional to $exp(-1/B)$ which appears at higher fields. This behavior is in agreement with a description of vortex dynamics with a Langevin equation of motion.

One of the more puzzling features of high-temperature superconducting oxides is the observation of large relaxation effects in the magnetization [1]. It is reasonably obvious that two key ingredients involved in the understanding of this phenomenon are the small coherence length [2] and the high temperatures, resulting in vortex pinning energies which are small compared to the energy of thermal fluctuations. As a consequence, a successful vortex dynamics in high-temperature superconducting films needs to incorporate these two essential features. In this communication we report measurements of the vortex impedance Z_v of $YBa_2Cu_3O_7$ (YBCO) films exposed to weak ($B << H_{c2}$) perpendicular magnetic fields. We interpret our results with a model where individual vortices execute overdamped brownian motion in a sinusoidal pinning potential.

Thin films (tickness $d < 1000\mathring{A}$) of YBCO were deposited onto single crystal $SrTiO_3$ (100) substrates using a single target hollow cathode magnetron [3]. Standard characterization of the films included X-ray diffractometry, Rutherford backscattering spectroscopy and measurements of the dc resistive and of the ac inductive zero-field transitions [4,5]. The best films were c-axis oriented, had very sharp ac and dc transitions (transition widths $< 2K$) at $\sim 90K$, a resistivity ratio of $R(300K)/R(90K) \simeq 3$, and critical current densities of $\sim 10^6 A/cm^2$ at $77K$. With decreasing film thickness a decrease in the transition temperature T_c was observed, $200\mathring{A}$ thick films having a T_c around $80K$. The complex sheet impedance $Z = R + i\omega L$ of the films was measured with a two-coil mutual inductance technique [6] in perpendicular magnetic fields ranging from "zero" (reduced to a few mG with μ-metal shielding) to $0.5T$ at a measuring frequency of, typically, $3kHz$.

Figure 1 shows the magnetic field dependence of the real and imaginary parts of Z at various temperatures not too far below T_c. In order to improve the measurement sensitivity [6], these data were taken on a very thin ($200\mathring{A}$) film with $T_c = 78K$ and a normal state sheet resistance $R_\square = 220\Omega$ at $T = 85K$. The lag in response due to vortex pinning, as measured by

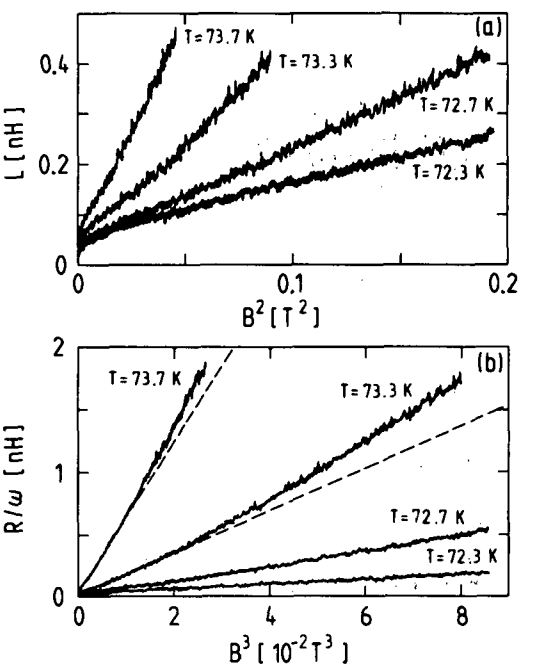

Figure 1: a) Imaginary part L and b) real part R/ω of the complex sheet impedance as a function of magnetic field B at various temperatures. Straight dashed lines in b) emphasize the deviation from the B^3-dependence at high temperatures.

$L(B)$ shown in Fig. 1a, depends linearly on B^2 with a temperature-dependent zero-field intercept $L(0)$, which is the kinetic inductance $L_k(T)$ of the superfluid background. The real part of the impedance (Fig. 1b) is proportional to B^3, with an upward deviation from linearity at higher temperatures.

In order to explain these results, we write for the to-

tal complex sheet impedance $Z = i\omega L_k(T) + Z_v(T,B)$ where, at our low fields, L_k is assumed independent of B. For the derivation of an expression for the vortex contribution $Z_v(T,B)$ to Z, we notice that the vortex lattice in YBCO, especially at temperatures close to T_c, is very soft because of the large magnetic field penetration depth [7]. It thus seems appropriate to neglect the interaction between the vortices in the lattice and consider a single vortex dynamics based on the following one-dimensional Langevin equation of motion

$$m\ddot{x} = -\eta\dot{x} - \frac{\delta U}{\delta x} + f(t) \qquad (1)$$

where m is the vortex mass, $\eta = \phi H_{c2}/R_\Box$ the viscosity coefficient [8], $U(x)$ the pinning potential and $f(t)$ an uncorrelated stochastic force satisfying $< f(t)f(0) >= 2\eta kT\delta(t)$, the angled brackets denoting averaging over time. We assume a periodic pinning potential of the form $U = U_0(1 - cosqx)$, where q^{-1} is a characteristic pinning length scale and $U_0 \simeq \phi_0^2 j_{c0}/B$ [9] is the amplitude of the pinning potential, with j_{c0} the zero-field critical current density. With a continued fraction expansion [10] it is possible, in the overdamped limit, to derive from Eq. (1) an ac vortex mobility corresponding to

$$Z_v = R_f\{1 + \frac{I_0^2(z) - 1}{1 - i\omega\tau[I_0^2(z) - 1]I_0(z)/I_1(z)}\}^{-1}, \qquad (2)$$

where $R_f = B\phi_0/\eta$ is the sheet flux flow resistance, $\tau = \eta/(U_0 q^2)$ the characteristic time for viscous relaxation of a vortex, I_n a modified Bessel function of order n and $z = U_0/kT$. Except very close to T_c the conditions $\omega\tau \ll 1, z \gg 1$ are satisfied, leading to the approximation

$$R = R_f[(\omega\tau)^2 + \frac{1}{I_0^2(z)}] \quad , \quad L = L_k + R_f\tau[1 - \frac{1}{I_0^2(z)}] \qquad (3)$$

At low enough temperatures the contributions arising from thermal fluctuations are exponentially small $(1/I_0^2 \simeq 0)$ so that, with the mentioned expressions for τ, R_f and U_0, Eq. (3) predicts the magnetic field dependences observed in Fig. 1: $L \propto B^2$ and $R \propto B^3$. As the temperature increases, fluctuation effects make the second term in the expression for R non-negligible, leading to the deviations from linearity observed in Fig. 1b. These deviations are expected to be $\propto exp(-1/B)$, since for large z the Bessel function can be approximated with an exponential. This behavior is observed in Fig. 2, where, on a logarithmic scale, the quantity $\Delta(R/\omega) \equiv R/\omega - R_f\omega\tau^2$ is plotted versus inverse magnetic field, at the temperature $73.3K$. From the slope of the dashed line, and the expression for U_0, we deduce $j_{c0} = 3.10^4 A/cm^2$, in good agreement with $j_{c0} = 6.10^4 A/cm^2$, as inferred from transport measurements in similar films at the same reduced temperature.

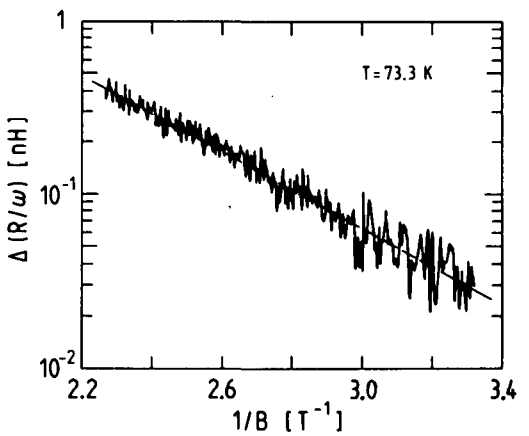

Figure 2: Difference between measured R/ω values and the linear fit (dashed line) of Fig. 1b at $73.3K$ as a function of inverse magnetic field. The slope of the dashed line yields a zero field critical current density $j_{c0} = 3.10^4 A/cm^2$.

The last term in the expression for L becomes appreciable only at even higher temperatures, i.e. close to T_c, where large dissipative effects make the extraction of L from the data a difficult problem [6]. Nevertheless, just below T_c we find that $L(B)$ deviates downward from the B^2-dependence at high fields, in qualitative agreement with Eq. (3).

An extension of the present measurements to high magnetic fields is in progress and will be published elsewhere, together with a detailed presentation of the vortex dynamics outlined above.

This work was supported by the Swiss National Science Foundation.

References

* Present Address: Laboratorium für Festkörperphysik, ETH Hönggerberg, 8093 Zürich
1. K.A. Müller et al, Phys. Rev. Lett. 58, 1143 (1987)
2. T.K. Worthington et al, Phys. Rev. Lett. 59, 1160 (1987)
3. X.X. Xi et al, J. Less Common Metals 151, 349 (1989)
4. P.K. Srivastava et al, IEEE Trans. Magn. MAG-25, 2575 (1989)
5. Ph. Flückiger et al, Physica C 162-164, 1563 (1989)
6. B. Jeanneret et al, Appl. Phys. Lett. 55, 2336 (1989)
7. E.H. Brandt, J. Low Temp. Phys. 26, 709 (1977)
8. J. Bardeen and M.J. Stephen Phys. Rev. 140, A1197 (1965)
9. M. Tinkham, Phys. Rev. Lett. 61, 1658 (1988)
10. W. Dietrich et al, Z. Physik B 27, 177 (1977)

MAGNETOCONDUCTANCE OSCILLATIONS IN HIGH TEMPERATURE SUPERCONDUCTING NETWORKS

Ph. Flückiger, V. Marsico, P.K. Srivastava,
Ch. Leemann, and P. Martinoli,
Institut de Physique, Université de Neuchâtel,
2000 Neuchâtel, Switzerland

Abstract

The complex ac impedance Z of superconducting $YBa_2Cu_3O_7$ triangular networks exposed to a perpendicular magnetic field was measured with a two coil mutual inductance technique. At temperatures close to the transition temperature, both the imaginary and the real part of Z as a function of the magnetic field show oscillations resulting from flux quantization in the unit cell of the network.

Introduction

Superconducting wire networks provide excellent model systems to study general concepts of two-dimensional condensed matter and fundamental material properties such as penetration depth, coherence length and vortex pinning potential. Furthermore, fabrication by photolithographic techniques of high temperature superconducting networks represents an important technological step towards the integration of high temperature superconducting microstructures in electronic devices.

Flux quantization phenomena in $YBa_2Cu_3O_7$ wire networks have previously been observed with resistive measurements[1]. In this paper we present the first measurements of the magnetoconductance oscillations in high temperature superconducting networks. Our two coil mutual inductance technique[2,3] allows a direct measurement of the complex ac impedance Z of the network and is thus much more sensitive in the sample's superconducting state than dc resistive measurements.

Sample Fabrication

The films were sputtered onto (100) $SrTiO_3$ single crystal substrates with an in situ (no post annealing) process using a single target hollow cathode magnetron[4]. The substrate temperature was held at 830C. The sputtering gas was a mixture of oxygen and argon in a 1:4 ratio and the total pressure was 0.6mbar. The plasma dc current was 0.2 A at 135 V giving a deposition rate of approximately 1 $\AA$/s at a distance of 1cm from the target. After the deposition the system was filled with pure oxygen and the film cooled to 450C in 15 seconds. It was annealed there for 5 minutes and cooled further to room temperature in 2 minutes. As calibrated by Rutherford backscattering spectrometry the film thickness was $d = 1000\AA$ and there was no interdiffusion between the film and the substrate. X-ray analysis revealed a film orientation with the c-axis perpendicular to the substrate. The superconducting transition of a film as seen in a resistive four-probe measurement is presented in Fig.1. Above T_c the behavior is clearly

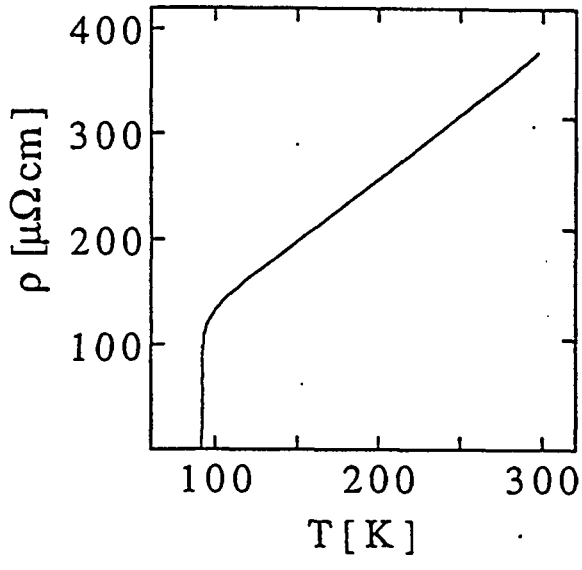

Figure 1. Temperature dependence of the dc resisivity of a $YBa_2Cu_3O_7$ thin film, c-axis oriented and $1000\AA$ thick.

metallic. The normal state resistivity near T_c was estimated to be around $120\mu\Omega cm$ and the resistivity ratio $\rho(300K)/\rho(100K)$ is found to be 2.8. The transition width (90% – 10%) is about 1K and the film becomes fully superconducting at about $91.4K$. Photoresist $2.5\mu m$ thick was then spinned onto the film and exposed through a contact mask fabricated by electron beam lithography. After developing the photoresist, triangles of $YBa_2Cu_3O_7$ were removed by ion beam etching with 2kV argon ions. Fig.2 shows an optical (a) and a scanning electron (b) micrograph of a portion of the resulting network of $\sim 10^6$ nodes, where we observe inhomogeneities in the geometry of the links. The lattice parameter and the wire width were $a = 5\mu m$ and $w = 1\mu m$ respectively. After this patterning process the zero-resistance temperature of the array was found to be 83.3K, which represents a T_c degradation of $8.1K$ probably caused by the ion beam etching.

Results and Discussion

The impedance of the networks was measured with a two-coil mutual inductance technique[2,3]. The detector consisting of an external drive coil and an internal concentric gradiometric receive coil was placed directly

Manuscript received September 24, 1990.

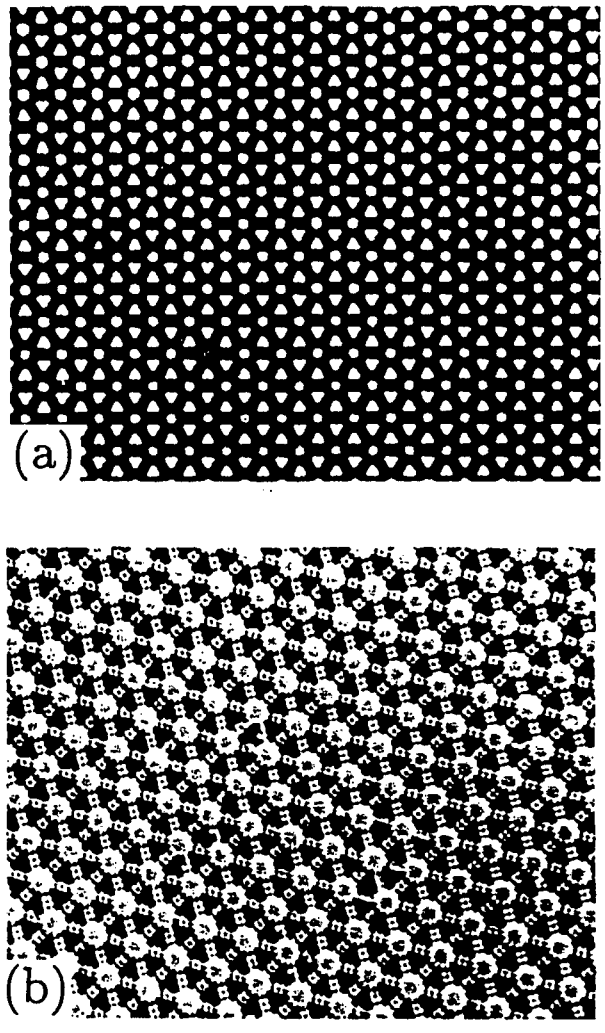

Figure 2. Optical (a) and scanning electron (b) micrographs showing a portion of a network consisting of 10^6 nodes. The lattice parameter is $a = 5\mu m$.

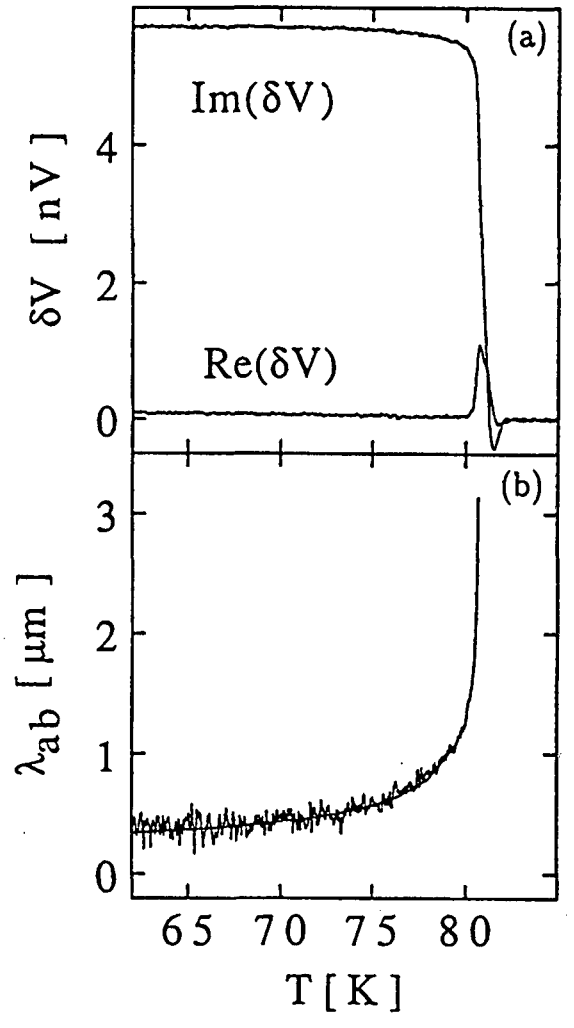

Figure 3. (a) Temperature dependence of the imaginary and real part of the response δV of the network. (b) Temperature dependence of λ_{ab} as determined from Fig.3 (a). Solid line: Fit by the London expression.

on the sample. An ac current of amplitude $I_D = 15\mu A$ and frequency $\nu \sim 3kHz$ (typical value) flowing through the drive coil generates screening currents in the network. The signal voltage δV at the receive coil induced by the screening currents was phase-sensitively detected by a conventional lock-in technique. Fig.3 (a) shows the real and the imaginary part of the response δV of the array at $1kHz$ as a function of the temperature. Using a numerical inversion procedure[3] it is possible to extract $Z = R + i\omega L_k$ from this signal where L_k is the kinetic inductance and R a resistance including all sources of dissipation: normal currents, flux motion and phase fluctuations. The kinetic inductance of the triangular network is directly related[3] to the bulk in plane penetration depth λ_{ab} by the following relation: $\lambda_{ab} = [dL_k\sqrt{3}w/(\mu_o a)]^{1/2}$. Fig.3 (b) shows the temperature dependence of λ_{ab} extracted from Fig.3 (a). The solid line in Fig.3 (b) is a fit to the London expression of the penetration depth[5,6] and provides the following parameters: $T_{co} = 81.2K$ and $\lambda_{ab}(T = 0K) = 2500\mathring{A}$. This value for λ_{ab} is not far from $1400\mathring{A}$ obtained in the best thin films and single crystals[7]. The fit is in good agreement with measurements up to $\sim 80K$. Above $80K$ the measured λ_{ab} diverges faster than the fit, an effect due to percolation of superconductivity between the grains present in the material[8].

In presence of a perpendicular magnetic field B the repulsive interaction between field-induced vortices tending to create a regular Abrikosov lattice is in competition with the pinning force provided by the network except when the two periodicities are matched. In this last situation the pinning of vortices is increased and thus the dissipative part R/ω presents a minimum and $1/L_k$, proportional to the superfluid density[9], presents a maximum. In Fig.4 $1/L_k$ and R/ω of the network at $6kHz$ are shown as a function of the frustration parameter $f = \Phi/\Phi_o$ expressing the applied flux per unit cell

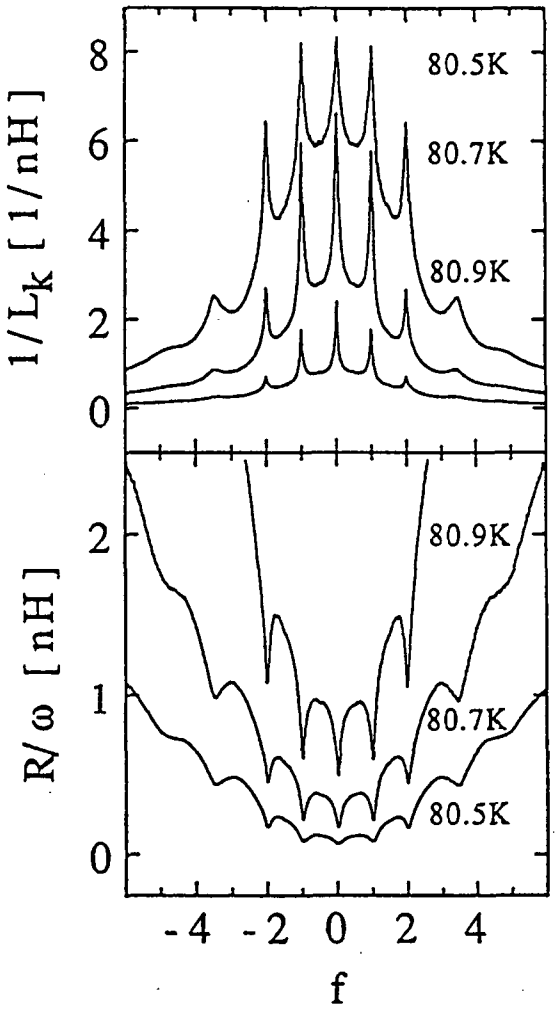

Figure 4. Inverse kinetic inductance $1/L_k$ and dissipative part R/ω of a $YBa_2Cu_3O_7$ network as a function of the frustration parameter f at different temperatures.

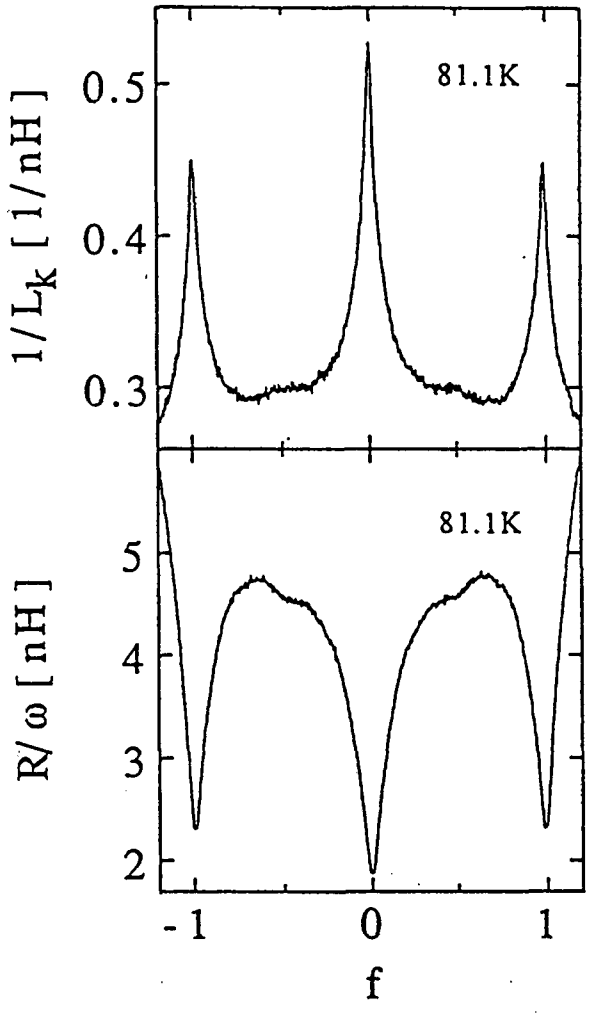

Figure 5. Expanded view of the inverse kinetic inductance $1/L_k$ and dissipation R/ω versus frustration showing structures at $f = 1/2$.

$\Phi = (\sqrt{3}/4)a^2B$ in units of the superconducting flux quantum Φ_o. Some oscillations corresponding to integer numbers of flux quanta per unit cell of the array are visible only in a very narrow region of about $0.4K$ below T_c and persist out to $f \sim 4$. A shift of the third and fourth peak towards higher fields can be observed but is not understood at this time. In Fig.5 we focus our attention on the frustration interval $[-1, 1]$ and we observe the appearance of structures at $|f| = 1/2$ indicating superconducting phase coherence over at least two unit cells.

In the following we compare the amplitude of the measured oscillations of $L_k^{-1}(f)$ with theoretical predictions. Neglecting phase fluctuations[10] and percolative effects[9] we assume: $L_k^{-1}(T, f) \sim [T_c(f) - T]$. Therefore we can write the following expression:

$$\frac{\Delta L_k^{-1}(T,f)}{L_k^{-1}(T,0)} = \frac{\Delta T_c(f)}{T_{co}}(1 - T/T_{co})^{-1} \qquad (1)$$

where $\Delta L_k^{-1}(T,f) \equiv L_k^{-1}(T,0) - L_k^{-1}(T,f)$ and $\Delta T_c(f) \equiv T_{co} - T_c(f)$. We can estimate $\Delta T_c(f)$ from two different models[11]: the linearized Ginzburg Landau (GL) theory and the mean field approximation of the XY model.

Considering first our triangular array as a network of "compact" superconducting wires we use the linearized GL theory and obtain the following result[12]:

$$\frac{\Delta T_c(f)}{T_{co}} = \frac{\xi^2(0)}{a^2}\arccos^2[\frac{E(f)}{6}] \qquad (2)$$

where $\xi(0)$ is the coherence length at $T = 0K$ and $E(f)$ the lowest eigenvalue of the linearized GL equation. Introducing[13] $E(0) = 6$ and $E_{min}(f) \simeq 2.7$ and assuming[1] $\xi(0) \simeq 13\mathring{A}$ we can estimate, using Eqs.1 and 2, the maximum relative variation of L_k^{-1}:

$$[\frac{\Delta L_k^{-1}}{L_k^{-1}}]_{max} = \frac{\xi^2(T)}{a^2}\arccos^2[\frac{E_{min}(f)}{6}] \qquad (3)$$

where $\xi^2(T) = \xi^2(0)(1 - T/T_{co})^{-1}$. For $T = 80.7K$ we find $[\Delta L_k^{-1}/L_k^{-1}]_{max} = 1.3 \cdot 10^{-5}$, a value which is 4 orders of magnitude smaller than the measurement presented in Fig.4!

As suggested by the scanning electron micrograph, it is probably more appropriate to picture the network as consisting of an assembly of islands weakly coupled by links forming Josephson junctions. This leads to the XY model and yields[11,13] the following expression for $E(f)$:

$$E(f) = \frac{2kT_c(f)}{E_J[T_c(f)]} \quad (4)$$

where $E_J(T)$ is the temperature-dependent coupling energy between two nodes of the array. Using the relation $E_J(T) = \hbar i_c(T)/2e$ and the Ambegaokar-Baratoff[6] expression of the critical current $i_c(T)$ we find:

$$\frac{\Delta T_c(f)}{T_{co}} = 0.54 \frac{R_s}{R_u} \frac{1}{E(f)} \quad (5)$$

where $R_u = \hbar/e^2 = 4.11k\Omega$ and R_s is the link resistance. Finally, using Eqs.1 and 4, we obtain:

$$[\frac{\Delta L_k^{-1}}{L_k^{-1}}]_{max} = 0.54 \frac{R_s}{R_u}(1 - \frac{T}{T_{co}})^{-1}[\frac{1}{E_{min}} - \frac{1}{E(0)}] \quad (6)$$

For $T = 80.7K$ and taking $R_s = 60\Omega$, as derived from dc resistive measurements of the film, we find a maximum relative variation $[\Delta L_k^{-1}/L_k^{-1}]_{max} = 0.26$ which is 2.2 times smaller than the measurement in Fig.4. This relatively small difference could be explained by thermal fluctuations in the form of vortices and domain walls which are not included in the mean field XY model or simply by a larger link resistance due to resistivity enhancement during patterning process. In our case the analysis developed in the framework of a Josephson coupled network seems thus appropriate.

Conclusions

The complex ac impedance of $YBa_2Cu_3O_7$ wire networks exhibits an oscillatory behavior reflecting flux quantization in the loops of the network. The difficulty to see structures at non integer rational f and the limited number of oscillations observed are probably an indication of reduction of the superconducting phase coherence by disorder and inhomogeneities in the network, as already suggested by the scanning electron micrograph.

Our work was supported by the Swiss National Science Foundation.

References

1. P. L. Gammel, P. A. Polakos, C. E. Rice, L. R. Harriott and D. J. Bishop, "Little-Parks Oscillations of T_c in Patterned Microstructures of the Oxide Superconductor $YBa_2Cu_3O_7$: Experimental Limits on Fractional-Statistics-Particle Theories", *Phys. Rev.*, B41, 2593-2596, 1990.

2. A. T. Fiory, A. F. Hebard, P. M. Mankiewich and R. E. Howard, "Penetration Depths of High T_c Films Measured by Two-Coil Mutual Inductances", *Appl. Phys. Lett.*, 52, 2165-2167, 1988.

3. B. Jeanneret, J. L. Gavilano, G.-A. Racine, Ch. Leemann and P. Martinoli, "Inductive Conductance Measurements in Two-Dimensional Superconducting Systems", *Appl. Phys. Lett.*, 55 2336-2338, 1989.

4. X. X. Xi, G. Linker, O. Meyer and J. Geerk, "Preparation of $YBa_2Cu_3O_{7-\varepsilon}$ Thin Films by Inverted Cylindrical Magnetron Sputtering", *J. Less-Common Met.*, 151, 349-355, 1989.

5. M. Tinkham, "Introduction to Superconductivity", McGraw-Hill, Inc., New York, 1975.

6. B. Mühlschlegel, "Die Thermodynamischen Funktionen des Supraleiters", *Z. Phys.*, 155, 313-327, 1959.

7. D. R. Harshman, L. F. Schneemeyer, J. V. Waszczak, G. Aeppli, R. J. Cava, B. Batlogg, L. W. Rupp, E. J. Ansaldo and D. Li. Williams, "Magnetic penetration depth in single-crystal $YBa_2Cu_3O_{7-\delta}$", *Phys. Rev.*, B39, 851-854, 1989.

8. Ch. Leemann, Ph. Flückiger, V. Marsico, J. L. Gavilano, P. K. Srivastava, Ph. Lerch and P. Martinoli, "Percolative Behavior of the Superconducting Transition of $YBa_2Cu_3O_7$ Films", *Phys. Rev. Lett.*, 64, 3082-3085, 1990.

9. J. E. Mooij, "Two-Dimensional Transition in Superconducting Films and Junction Arrays", in Percolation, Localization and Superconductivity, A.M. Goldman and S.A. Wolf, Ed., Plenum, New York, 1969.

10. B. Jeanneret, Ph. Flückiger, J. L. Gavilano, Ch. Leemann and P. Martinoli, "Critical Phase Fluctuations in Superconducting Wire Networks", *Phys. Rev.*, B40, 11373-11377, 1989.

11. Q. Niu and F. Nori, "Theory of Superconducting Wire Networks and Josephson Junction Arrays in Magnetic Fields", *Phys. Rev.*, B39, 2134-2150, 1989.

12. B. Pannetier, J. Chaussy, R. Rammal and J. C. Villegier, "Experimental Fine Tuning of Frustration: Two Dimensional Superconducting Network in a Magnetic Field", *Phys. Rev. Lett.*, 53, 1845-1848, 1984.

13. W. Y. Shih and D. Stroud, "Two-Dimensional Superconducting Arrays in a Magnetic Field: Effects of Lattice Structures", *Phys. Rev.*, B32, 158-165, 1985.

High T_c Superconductor Thin Films
L. Correra (Editor)

Growth and patterning of $Y_1Ba_2Cu_3O_7$ films

P. K. Srivastava, Ph. Flückiger, Ch. Leemann and P. Martinoli

Institut de Physique, Université de Neuchâtel, 2000 Neuchâtel, Switzerland.

Abstract

Highly c-axis oriented films of $Y_1Ba_2Cu_3O_7$ have been prepared by dc inverted cylindrical magnetron sputtering onto single crystal $SrTiO_3$ (100) substrates. These films have a superconducting transition temperature T_c of 90K, a very narrow transition width (1K), a resistivity ratio of $\rho(300K)/\rho(90K) = 3$ and critical current densities of $10^6 A/cm^2$ at 77K. Triangular and square wire networks consisting of 10^6 nodes with a periodicity of $5\mu m$ and line width of $1\mu m$ have been prepared on these films. The details of the deposition parameters and the fabrication of the wire networks are reported. Also, we will report the measurements of the complex ac impedance Z with a two coil mutual inductance technique from which the in-plane penetration depth was determined. Near the transition temperature, where vortex pinning is relatively weak, both the real and imaginary parts of Z show oscillations in a perpendicular magnetic field, resulting from flux quantization in the cells of the network.

1. Introduction

In order to be able to use superconducting oxide films in device fabrication it is essential for the films to have the right stoichiometry, right crystal structure, smooth surface, sharp interface between film and substrate, high superconducting transition temperature, small transition width and high critical current density at 77K. Among the different techniques which have been used for the deposition of superconducting oxide films, sputtering is the most common one. Both dc and rf sputtering using single or multiple targets in the planar magnetron mode have been employed. It has been observed that the film composition often deviates from the target composition due to the different sputtering rates of the constituents of the target and due to the bombardmemt of the negative ions emerging from the target resulting in selective resputtering. Many workers have overcome this problem by suitably adjusting the target composition or by using unconventional sputtering geometries[1-3]. A simple way to circumvent this problem, as used by Geerk [4], is to make films in a high sputtering gas pressure using an inverted cylindrical magnetron with a single composite target of $Y_1Ba_2Cu_3O_7$. We have used this technique to make superconducting oxide films of $Y_1Ba_2Cu_3O_7$ and have used these films for making superconducting networks with contact photolithography and ion milling. In this report we present fabrication and characterization of our films and measurements of flux quantization phenomena in $Y_1Ba_2Cu_3O_7$ networks.

2. Experimental details

A high vacuum chamber fitted with a turbo-molecular pump was used for the deposition of $Y_1Ba_2Cu_3O_7$ films on $SrTiO_3$ (100) substrates. A single stoichiometric target of composition Y:Ba:Cu in a 1:2:3 ratio was used. The target was of hollow cylindrical form having 3.0 cm inner diameter, 3.0 cm height and 0.5 cm wall thickness. It was mounted vertically, with the substrate on its heater at a distance of 2.0 cm below the target. Before each run the substrate heater was cleaned and outgassed at 980C for 2 hours in 10^{-6} Torr. The substrate was then mounted and cleaned at 900C for 1 hour in pure oxygen. Again the system was evacuted to the 10^{-6} Torr range, then the turbo-molecular pump was switched off and the rotary pump directly connected to the system. Two flowmeters, a mass-flow ratio controller and a pressure controller were used to maintain the desired sputtering pressure and an oxygen to argon ratio of 1:6. The substrate temperature was controlled by a programmable temperature controller and measured with a 0.5mm thick chromel-alumel thermocouple mounted in the substrate holder 0.2mm below the substrate. Due to the positioning of the thermocouple in the heater we believe that the real temperature of our substrate could be 50C to 100C lower than the measured value. After attaining the desired substrate temperature, the dc power supply was switched on for the deposition of the film. The various sputtering parameters used are: nominal substrate temperature between 800C and 900C, sputtering current 0.2A which developed a dc voltage 125V. After the deposition, the system was filled with pure oxygen and the films cooled to 450C in 15 sec. They were annealed for 5 minutes and cooled further to room temperature in 2 minutes. Typical film thicknesses as measured by Rutherford backscattering spectroscopy (RBS) are 200Å - 2000Å. The films as produced are black and shiny are microscopically smooth exhibiting a featureless microstucture as observed by optical microscopy. Observation with a scanning electron microscope (SEM) reveals a slightly grainy structure on a scale of 1000Å, as shown in figure 1.

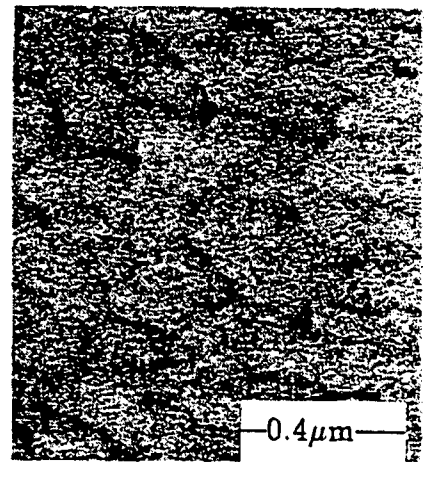

Fig. 1: SEM micrograph of a c-axis oriented film showing a smooth surface with some structure on a scale of 1000Å.

3. Results and Discussions

We have observed that along with other sputtering parameters, substrate temperature, Ar/O_2 ratio, power applied to the target and the cooling rate after the growth of the films play an important role in determining the crystal structure and the superconducting

properties of the films. X-ray diffraction of a film produced as described, with the substrate at 890C (figure 2(a)) shows the presence of a number of $(00l)$ peaks suggesting that the major phase consists of grains with the c-axis perpendicular to the film surface. For another film, prepared with an oxygen to argon ratio of 1:1 at a substrate temperature of 830C and slowly cooled from 830C to 450C (about 30 minutes), the presence of only (100) and (200) diffraction peaks with relatively large intensities (figure 2(b)) suggests a preferred grain growth with the a-axis perpendicular to the film surface. The parameters determining the good overall quality of our films, namely correct composition and c-axis orientation, appear to be substrate temperature, oxygen to argon ratio and a fast cooling rate.

The RBS spectrum of a c-axis oriented film along with a numerically calculated spectrum for a film with a thickness of 1600$\AA$ is shown in figure 3. From the step heights we calculate the composition of the film which in this case turns out to be Y:Ba:Cu in a ratio 1.6:2.0:3.0 The important feature of this data is the sharpness of the spectrum which suggests a sharp interface, without excessive intermixing or diffusion of film material into the substrate material.

The resistivity vs temperature curve for a good quality sample, as measured by a four probe method using indium as a contact material, is shown in figure 4. The $\rho(300K)/\rho(90K)$ ratio for the film is 3.0 and its resistivity at 95K is 110$\mu\Omega$cm. The transition temperature is 90K and the transition width about 1K. For the critical current density measurements we have fabricated 40μm wide and 500μm long strips with wet chemical etching. A voltage criterium of 0.2 μV was used for the measurement of the critical current. As shown in figure 5, this film has a critical current density at 77K in excess of 10^6 A/cm^2.

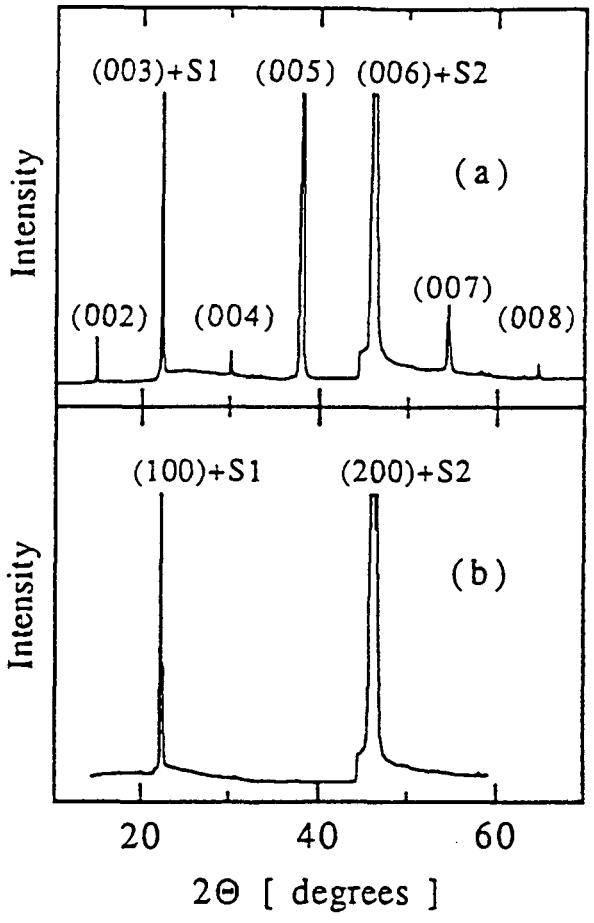

Fig. 2: X-ray diffraction pattern (a) of c-axis oriented and (b) a-axis oriented films. S1 and S2 are the (100) and (200) lines of (100) oriented $SrTiO_3$ substrate.

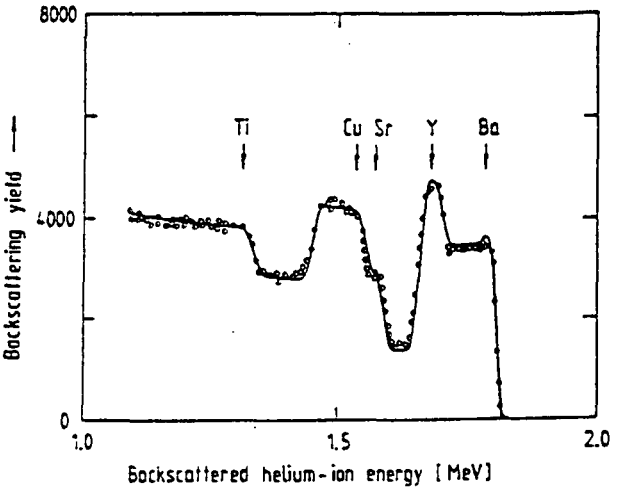

Fig. 3: RBS spectrum of a c-axis oriented film. Circles are the measured spectrum, full line is the spectrum calculated for a $Y_{1.6}Ba_{2.0}Cu_{3.0}O_{6.0}$ film of thickness 1600$\AA$.

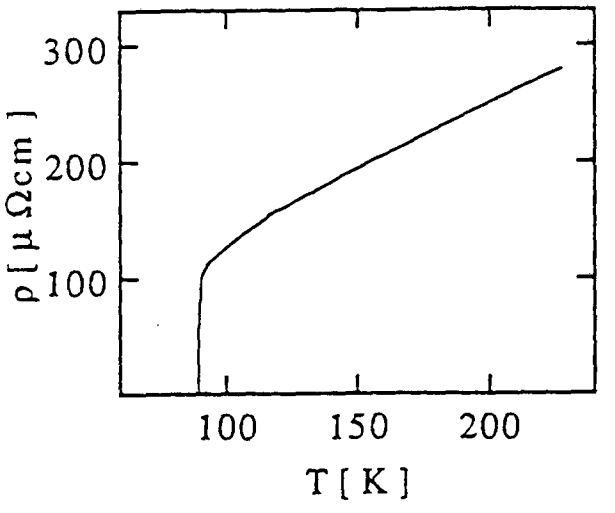

Fig. 4: Temperature dependence of the dc resistivity of good quality film showing metallic behaviour above the transition temperature and a narrow transition width at 90K.

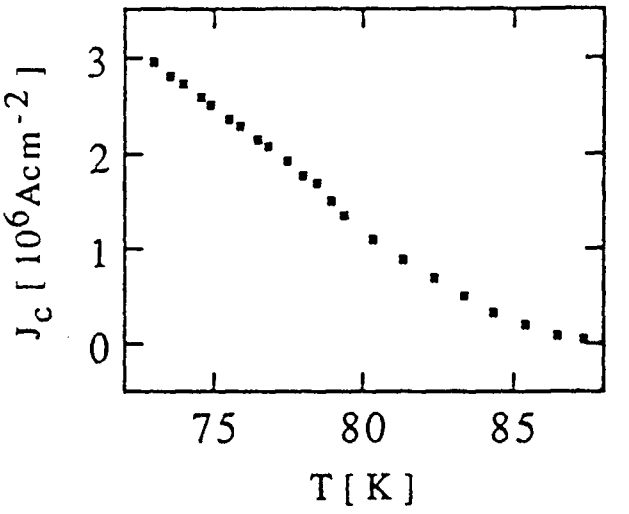

Fig. 5: Temperature dependence of the critical current density of a c-axis oriented thin film.

The penetration depth of the films was deduced from inductive conductance data as measured with a two coil mutual inductance method described in earlier papers [5-8]. Basically it is an eddy current technique. The sample is positioned directly under a coil assembly consisting of an excitation coil and a concentric gradiometer detection coil. A current flowing in the excitation coil induces sreening currents in the film which in turn induce a signal (δV) in the detection coil which can be phase senstively detected. The variation of the in phase Re(δV) and quadrature component Im(δV) of the signal with temperature for a c-axis film is shown in figure 6. With a numerical inversion procedure [8] we can extract from the signal (δV) the complex impedance of the film Z= R + iωL_k , where R is the resistance and L_k the sheet kinetic inductance. The penetration depth λ [8] is directly connected to the L_k by the relation $L_k = \mu_0\lambda^2/d$ where d is the thickness of the film. From a fit to the London expression for λ, with the mean field transition temperature and $\lambda(0)$, the penetration depth at zero temperature, as adjustable parameters, we find, for our best films, $\lambda(0)$=2500$\AA$, not far from 1400$\AA$ obtained for single crystal thin films [9].

Triangular and square networks with lattice parameter a = 5μm and wire width w = 1μm were fabricated on c-axis oriented

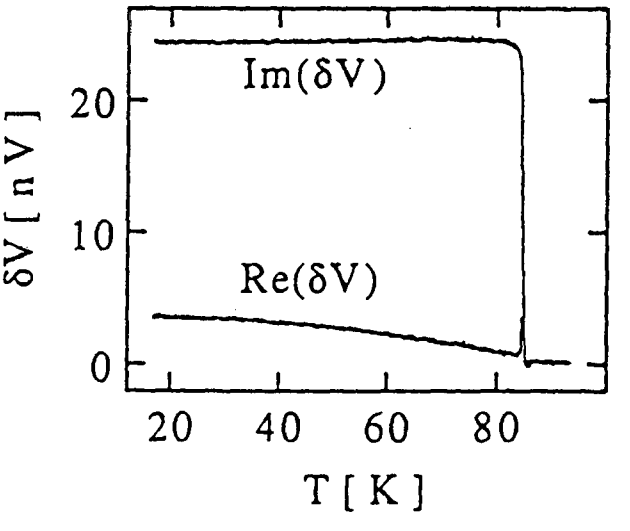

Fig. 6: Temperature dependence of the measured signal Im(δV) and Re(δV) from which the thin film penetration depth can be extracted.

films with contact photolithography and argon ion milling. First photoresist 2.5μm thick was spinned onto the film and exposed through a contact mask fabricated by electron beam lithography. After developing the photoresist, the unwanted $Y_1Ba_2Cu_3O_7$ was removed by ion milling with 2kV argon ions. An SEM mircograph of a resulting network, consisting of $\sim 10^6$ nodes, is shown in figure 7. After the patterning process the superconducting transition temperature of the network was found to be 83.5K, this degration is due to the ion beam etching.

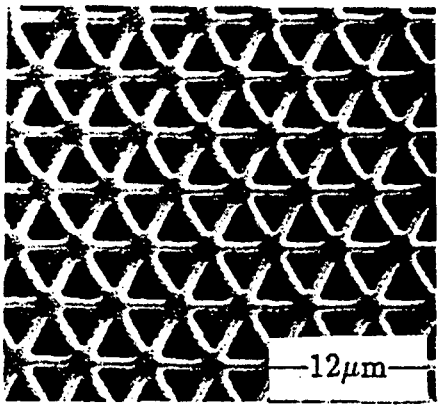

Fig. 7: SEM micrograph of a triangular network.

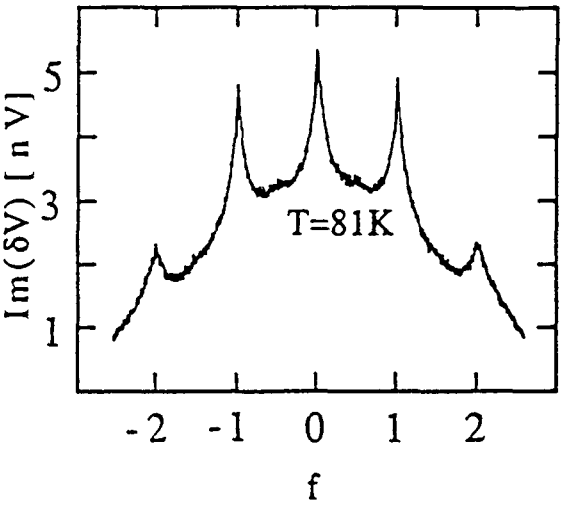

Fig. 8: Magnetoconductance oscillations of the network shown in figure 7 as a fuction of magnetic field

In the presence of a perpendicular magnetic field B the imaginary and real parts of the conductance of the networks show oscillations which are visible in a very narrow region of about 0.4K below the transition temperature. These oscillations are the result of flux quantization in the loops of the networks. In figure 8, Im(δV) of a triangular network measured at 6kHz is shown as a function of the frustration parameter $f = \Phi/\Phi_o$, expressing the applied flux per unit cell, $\Phi = \sqrt{3}a^2B/4$ in units of the superconducting flux quantum Φ_o. The oscillations observed correspond to integer numbers of flux quanta per unit cell of the network.

4. Conclusions

High temperature superconducting oxide films of $Y_1Ba_2Cu_3O_7$ have been prepared by dc cylindrical magnetron sputtering by utilizing high gas pressure and insitu annealing. By optimizing the substrate temperature, the cooling cycle and the oxygen to argon ratio in the sputtering gas, we have obtained good quality a-axis and c-axis oriented films. Further we have optimized the lithographic process to obtain triangular and square net-

works without substantially degrading the superconducting properties and have shown that these superconducting networks exhibit magnetoconductance oscillations in a perpendicular magnetic field.

Our work was supported by the Swiss National Science Foundation.

5. References

1. H. C. Li, G. Linker, F. Ratzel, R. Smithey and J. Geerk, Appl. Phys. Lett., 52 (1988) 1098.

2. R. L. Sandstrom, W. J. Gallagher, T. R. Dinger, R. H. Koch, R. B. Laibowitz, A. W. Kleinsasser, R. J. Gambino, B. Bumble and M. F. Chisholm, Appl. Phys. Lett., 53 (1988) 444.

3. H. Koinuma, M. Kawasaki, S. Nagata, K. Takeuchi and K. Fueki, J. Appl. Phys., 27 (1988) L376.

4. X. X. Xi, G. Linker, O. Mayer, E. Nold, B. Obst, F. Ratzel, R. Smithey, B. Strehlau, F. Weschenfelder and J. Geerk, Z. Phys. B, 74 (1989) 13.

5. P. K. Srivastava, P.Debély, H. E. Hintermann, Ch. Leemann, Ph. Flückiger, O. Caccivio, J. L. Gavilano, J. Weber and P. Martinoli, IEEE Trans. Magn., MAG-25 (1989) 2575.

6. P. K. Srivastava, P.Debély, H. E. Hintermann, Ph. Flückiger, J. L. Gavilano, Ch. Leemann, J. Weber and P. Martinoli, in *Surface Modification Technologies III*, edited by T. S. Sudarshan and D. G. Bhat (The Minerals, Metals and Material Society, Warrendale, PA, 1990) p. 219

7. A. F. Hebard and A. T. Fiory, Appl. Phys. Lett. 52 (1988) 2165.

8. B. Jeanneret, J. L. Gavilano, G. -A. Racine, Ch. Leemann and P. Martinoli, Appl. Phys. Lett., 55 (1989) 2336.

9. D. R. Harshman, L. F. Schneemeyer, J. V. Waszczak, G. Aeppli, R. J. Cava, B. Batlogg, L. W. Rupp, E. J.Ansaldo and D. Li, Phys. Rev., B39 (1989) 851.

11 Liste des publications

1. B. Jeanneret, Ph. Flückiger, J.L. Gavilano, Ch. Leemann and P. Martinoli.
   Critical Phase Fluctuations in Superconducting Wire Networks.
   Phys. Rev. B 40, 11374 (1989).

2. B. Jeanneret, Ph. Flückiger, Ch. Leemann and P. Martinoli.
   Dynamical Study of the Superconducting Phase Transition of Two-Dimensional Networks.
   IEEE Trans. Magn. MAG 25, 1428 (1989).

3. P.K. Srivastava, P. Debély, H.E. Hintermann, Ch. Leemann, Ph. Flückiger, O. Caccivio, J.L. Gavilano, J. Weber and P. Martinoli.
   Complex ac Conductance of YBaCuO Films.
   IEEE Trans. Magn. MAG 25, 2575 (1989).

4. P.K. Srivastava, P. Debély, H. Boving, H.E. Hintermann, Ph. Flückiger, Ch. Leemann, J. Weber and P. Martinoli.
   Growth of R.F. Magnetron Sputtered $Y_1Ba_2Cu_3O_7$ Thin Films.
   Proceedings of the 7th Int. Conf. on Ion and Plasma Assisted Techniques (IPAT 89, Genève), CEP Consultants Ltd (Edinburgh), 361 (1989).

5. Ph. Flückiger, J.L. Gavilano, Ch. Leemann, P. Martinoli, B. Dam, G.M. Stollman, P. K. Srivastava, P. Debély and H.E. Hintermann.
   Penetration Depth in YBaCuO Films.
   Physica C 162-164, 1563 (1989).

6. Ch. Leemann, Ph. Flückiger, V. Marsico, J.L. Gavilano, P.K. Srivastava, Ph. Lerch and P. Martinoli.
   Percolative Behavior of the Superconducting Transition of $YBa_2Cu_3O_7$ Films.
   Phys. Rev. Lett. 64, 3082 (1990).

7. P. Martinoli, Ph. Flückiger, V. Marsico, P. K. Srivastava, Ch. Leemann, and J.L. Gavilano.
   Vortex Dynamics in $YBa_2Cu_3O_7$ Films.
   Physica B 165&166, 1163 (1990).

8. Ph. Flückiger, V. Marsico, P.K. Srivastava, Ch. Leemann and P. Martinoli.
   Magnetoconductance Oscillations in High Temperature Superconducting Networks.
   IEEE Trans. Magn. MAG 27, 1612 (1991).

9. P.K. Srivastava, Ph. Flückiger, Ch. Leemann and P. Martinoli
   Growth and Patterning of $YBa_2Cu_3O_7$ Films.
   Article paru dans *High Tc Superconductor Thin Films*, proceedings of the International Conference in Advanced Materials (ICAM 91), édité par L. Correra, Elsevier Science Publishers, 377 (1992).